Journal of South American Earth Sciences 116 (2022) 103792

Contents lists available at ScienceDirect

Journal of South American Earth Sciences

journal homepage: www.elsevier.com/locate/jsames

Cenozoic ash-fall deposits in the Andean foreland basins, Northwest Argentina (23°-26°S) - Key to reconstruct their chrono-stratigraphy and to identify links to the Andean Neogene ignimbrite flare-up

Beatriz Coira [a,*], Claudia I. Galli [a,b], Suzanne Mahlburg Kay [c], Ricardo N. Alonso [d], Patrocinio Flores [e], Edgardo David González [a]

[a] Instituto de Ecorregiones Andinas (INECOA), CONICET-Universidad Nacional de Jujuy, Av. Bolivia 1661, (4600) S. S. de Jujuy, Argentina
[b] Facultad de Ciencias Naturales, Universidad Nacional de Salta, Av., Bolivia 5150, 4400, Salta, Argentina
[c] Department of Earth and Atmospheric Sciences, Cornell University, Ithaca, NY14853, USA
[d] CEGA-CONICET, Universidad Nacional de Salta, Campo Castañares, 4400, Salta, Argentina
[e] Instituto de Geología y Minería, Universidad Nacional de Jujuy, Av. Bolivia 1661, (4600) S. S. de Jujuy, Argentina

ARTICLE INFO

Keywords:
Cenozoic-ash-fall deposits- Andean foreland basins- Northwest Argentina
Chrono-stratigraphy

ABSTRACT

Outstanding Cenozoic ash-fall deposits have been recognized in Andean foreland basins in NW Argentina. The purpose of this contribution is to review their stratigraphic, petrographic, geochemical and geo-chronogical data in the Neogene deposits of the Andean foreland basins at 23°-26°S, between the Puna highland, to the west, and the fold thrust belt to the east. In doing this we evaluate their potential as chrono-stratigraphic markers, analyze the different volcanic events that they represent, evaluate them in relation to the Southern Central Andes volcanism and to determine the pattern of their distribution.

Different ash-fall events were recognized at 15-11 Ma; 10–6.8 Ma; 6.4 to 4.8; 4.3 to 2.6; and from 2.1-Ma-Recent across the Neogene foreland basins deposits. Mineralogical and geochemical data of the ash fall deposits were analyzed in each event in order to characterize them during the different pulses. Those data were evaluated with respect to those of the contemporary most voluminous explosive volcanism represented by the Neogene ignimbrite flare up of the Southern Central Andes to test the feasibility to identify their potential sources. The eruptive sources of these ash-fall events were identified as the Neogene giant calderas of the Altiplano Puna Volcanic Complex (APVC), and the Southern Puna (Agua Escondida, Luingo calderas/15-11 Ma; Cerro Aguas Calientes Caldera, Complejo Volcánico Negra Muerta, Ramadas Volcanic Center/10 Ma- 6.8 Ma; Galán and Puripicar calderas/6.4–4.8 Ma; Guacha, Pacana, Puripicar and Galán calderas/4.3–2.6 Ma; Purico Complex and Guacha Caldera 2.1 Ma-Recent. Comprehensive analysis of the ash-fall deposits, across the different basins in a W-E profile at same time has shown that their distribution is consistent with an east-southeast, and to a lesser extent, east northeast dispersion from the Neogene giant calderas as controlled by northwesterly and westerly winds.

These results indicate the effectiveness of using stratigraphy, mineralogy, geochemistry and ages in comparing ash-fall tuffs with coeval ignimbrites in order to correlate stratigraphic sequences in foreland basins, identify explosive volcanic events, contemporary emission centers and to put forward their dispersion patterns.

1. Introduction

Outstanding Cenozoic ash-fall deposits have been recognized in Andean foreland basins in NW Argentina. Such is the case in the Calchaquí, Amblayo, Lerma, Metán, Rio Grande Jujuy, Siancas, Humahuaca-Casa Grande basins between 23°S and 26°S, between the Puna plateau, to the west, and the fold thrust belt to the east. These basins are located east of the extended Neogene ignimbrite fields of one of the largest ignimbrite provinces on Earth. Those ash-fall deposits are recognized as far as 250–350 km to the southeast and north (Calchaquí,

* Corresponding author.
E-mail addresses: bcoira2015@gmail.com (B. Coira), cgalli@unsa.edu.ar (C.I. Galli), smk16@cornell.edu (S.M. Kay), rnalonso@gmail.com (R.N. Alonso), patro@idgym.unju.edu.ar (P. Flores), edgtoyo@gmail.com (E.D. González).

https://doi.org/10.1016/j.jsames.2022.103792
Received 11 January 2022; Received in revised form 25 March 2022; Accepted 28 March 2022
Available online 1 April 2022
0895-9811/

Lerma, Metán basins) and 200 km east and northeast (Humahuaca basin) of the Late Miocene-Quaternary ignimbrite deposits and giant calderas (Fig. 1) from near the Bolivian–Chilean and Argentine border (Altiplano–Puna Volcanic Complex, de Silva, 1989) and further east in the Puna back arc (Kay et al., 2010).

The ignimbrite flare-up in that region extend over ca. 10 Ma with emission of large ignimbrite volumes over 600–2000 km^3 associated with giant calderas with impressive dimensions of up to 60 × 35 km in diameter. These calderas include La Pacana, Guacha, Pastos Grandes, Laguna Colorada, Vilama, Panizos, Coranzulí, Aguas Calientes, Negra

Fig. 1. Satellite Radar Topography Mission (SRTM) image of the Southern Central Andean (21°30′-26°30′S) showing the Cenozoic Giant Calderas and their ignimbrites considered in the study region.

Muerta. La Amarga, La Escondida, Luingo, Galán and Cerro Blanco (Fig. 1). These major ignimbrite eruptions were produced in successive pulses that increased in intensity through time with pulses from ca 15-10 Ma to a waning stage from 2 Ma to Recent, (Coira et al., 1993; Kay et al., 1999, 2011; de Silva et al., 2006; de Silva and Gosnold 2007; Kay and Coira 2009; Kern et al. (2016).

The ages of the distal ash deposits recognized in the Neogene foreland basins in NW Argentina (23°-26°S) extend from the Miocene to Pleistocene with the oldest deposits at 15-11 Ma in the Calchaquí and Amblayo basins followed by a succession of peaks in the remaining basins until the waning stage at 2.2-Recent Ma. The ages of these ash deposits are concordant with the timing of the ignimbrite flare-up in the region in accord with these ash deposits being distal of the ignimbrite flare-up.

Ignimbrites generally have distal ash deposits originating from eruption columns of large Plinian eruptions or from ash-clouds

Fig. 2. Satellite Radar Topography Mission (SRTM) image of the Southern Central Andean (21°30′-26°30′S) with insets indicating location of detailed maps of the studied regions: 3 Calchaquí, Lerma, Metán basins (Fig. 4); 2 Rio Grande de Jujuy, Sianca, Lerma basins (Fig. 5); 1 Humahuaca–Casa Grande basins (Fig. 6).

elutriated from pyroclastic density currents (co-ignimbrite ash) (Sparks and Walker, 1977; Chesner et al., 1991). Given that, the ignimbrite flare-up deposits in the region generally lack ash fall deposits, these deposits could have been derived from co-ignimbrite ash clouds, as considered by Breitkreuz et al. (2014) in the Coastal Cordillera of northern Chile.

In this study we evaluate previous stratigraphic, textural, petrographic, geochemical and geo-chronological data from ash-fall deposits preserved in the Neogene sequences of the Andean foreland basins, throughout the region from 23°-26°S (Calchaquí, Amblayo, Lerma, Metán, Rio Grande de Jujuy, Siancas, Humahuaca, Casa Grande basins). We then use these data to comprehensively analyze the pattern of ash dispersion, their usefulness as chrono-stratigraphic markers and their link to the centers and events of the ignimbrite mega eruptions during their evolution.

2. Dispersion of cenozoic ashes in the NW foreland basins (Argentina)

The Andean foreland basins considered in this study are from 23° to 26°S, between the Puna highland, to the west, and the folded thrust belt to the east (Fig. 2). They are valuable archives of Andean Neogene ignimbrite flare-up with links to the arc and back arc mega-calderas that dispersed conspicuous volumes of ashes into the thick sedimentary filling of those basins.

The structural evolution of the Andean foreland basin was mainly controlled by the inversion of the extensional basins of the Cretaceous rift of the Salta Group that occurred as a thick to thin skinned fold thrust belt into the foreland in the Eocene-Oligocene and as foreland basins partitioned into intermontane basins in the Miocene. These basins include Calchaquí Tonco, Amblayo basins (Fig. 4), in which the Payogastilla Group deposits (Díaz y Malizzia, 1983) accumulated. Others are the Lerma, Metán, Rio Grande de Jujuy and Siancas basins in which the Orán Group (Russo, 1972) accumulated (Fig. 5). So too the Casa Grande basin in which the Casa Grande, Río Grande and Pisungo and Mal Paso Formations (Fernández et al., 1973) deposited during Upper Eocene-Upper Pliocen (Boll and Hernandez, 1986; Hernández et al., 1999; Kley et al., 2005) and the Humahuaca basin that contains the syn-orogenic deposits of the Maimará Formation (Upper Miocene-Lower Pliocene, Salfity et al., 1984) that accumulated in a fragmented foreland basin (Siks and Horton, 2011; Pingel et al., 2013 Galli et al., 2016), and those deposits Upper Pliocene e Lower Pleistocene of the Tilcara (Pingel et al., 2013)./Uquía Formation (Castellanos, 1950) and the Pleistocene deposits, accumulated in that intermontane basin (Galli et al., 2021).

In all these basins a continental sedimentary environment prevails, including an ephemeral fluvial system with aeolian dune fields; a sandy braided fluvial system; a playa lake; a sinuous gravelly sandy fluvial system with lagoons; and lagoons and marshes (Galli et al., 2014).

2.1. Intermountain basins

2.1.1. Calchaquí-Tonco–Amblayo intermountain basins

In the Calchaquí intermountain basin the Payogastilla Group deposits, integrated, from base to top, by the Los Colorados, Angastaco, Palo Pintado and San Felipe formations (middle-upper Eocene to middle Miocene, Díaz y Malizzia, 1983), recorded the evolution of the Cenozoic foreland basin in the region. Sedimentary filling of the basin began with the deposition of the Los Colorados Formation and was characterized by sheet-flood ephemeral fluvial deposits formed by unconfined and confined channels within dune fields in an arid region (Galli et al., 2014). The first ash-fall record in the basin was represented in this unit by a tuff level of 21 ± 0.8 Ma (U/Pb, zircon) intercalated with the upper aeolian deposits (del Papa et al., 2004; Bosio et al., 2009; Galli and Reynolds, 2012; del Papa et al., 2013).

During the middle Miocene the explosive volcanism increase its representation in the basin in the Angastaco Formation that contains a shallow, gravel-braided fluvial system associated with gravity flows, with thicknesses of 4550 m (Calchaquí river) to 1500 m (Tonco Valley). In this unit tuff levels were recognized at the base of the Calchaquí river profile (* 1 Fig. 4): Tuff 1 dated at 13.6 ± 0.1 Ma (U/Pb zircon, Galli et al., 2014) and at 15.26 ± 0.23 Ma U/Pb by Pereyra et al. (2008), Tuff 2 in 13,4 ± 0,4 Ma (Ar/Ar, biotite Grier, 1990; Grier and Dallmeyer, 1990) from the middle sections in the Tonco Valley (*2 Fig. 4):Tuff 7 dated at 13.7 ± 0.1 Ma U/Pb Galli et al., 2014), and in the Amblayo Valley (*3 Fig. 5): Tuff 8 dated at 13.7 ± 0.1 Ma U/Pb, Galli et al., 2014).

In the Palo Pintado Formation, which represents an upper Miocene fluvial system with intra-channel and over-bank deposits (Galli et al., 2011) a new pyroclastic event was registered at the base in the Calchaquí river section, where a tuff level Tuff 3 dated at 10.20 ± 0.11 Ma (K/Ar, Galli et al., 2011) was recognized. Another pulse was represented in this unit by two ash fall deposits with ages of 6.8 ± 0.1 Ma and 6.3 ± 0.1 Ma (U/Pb, zircon, Galli et al., 2014) respectively in the Quebrada El Estanque section(* 4 Fig. 4.), and two others near the top of Calchaquí river section (*1 Fig. 4) Tuff 4 dated at 5.27 ± 0.28 Ma (206 Pb/238U) by Coutand et al. (2006) and at 5.98 ± 0.32 Ma U/Pb, zircon by Bywater Reyes et al. (2010).

In the San Felipe Formation deposits, interpreted as braided alluvial fans associated with shallow gravelly braided fluvial system, a tuff level dated at 5.17 ± 0.23 Ma was recognized 135 m above the contact with the Palo Pintado Formation (Fig. 1 *5, Bywater Reyes et al., 2010). In Quebrada Payogastilla sections (*5 Fig. 4) another tuffs of San Felipe Formation were dated in 3.99 ± 0.15 Ma; 4.04 ± 0.26 Ma, 4.81 ± 0.17 Ma (U/Pb, zircon, Bywater Reyes et al., 2010) which represent a new pyroclastic event in the lapse 3.99 Ma −5.17 Ma.

2.1.2. Lerma, Metán, Rio Grande de Jujuy, Siancas basins

Towards the east of Calchaquí basin, the Lerma, Metán, Sianca, and Rio Grande, basins evolved contemporaneously with that basin, accumulating the Orán Group deposits (Russo y Serraiotto 1978) which are divided into the Metán Subgroup and the Jujuy Subgroup (Russo, 1972). In the Orán Group different pyroclastic events have also been preserved. The initial pyroclastic records, during middle Miocene were represented in Lerma and Metán basins by tuff levels intercalated in the intermediate unit of the Subgroup, the Anta Formation (Gebhard et al., 1974; Arias y Chávez Manrique, 1976). (Fig. 3), unit product of ephemeral clastic flows that deposited sand sheet under high-flow regime conditions (Galli et al., 2017). Those tuff levels, vitro-crystalline with biotite and minor hornblende, were dated at Alemania (Guayacán section, *7 Fig. 4) in 14.5 ± 1.4 Ma (zircon fission-track), at Río Piedras (*11 Fig. 4), in $^{40}Ar/^{39}Ar$ age of 13.95 ± 0.72 Ma (Galli et al., 1996) and at Gonzalez section (* 13 Fig. 4) in K/Ar age 13.2 ± 1.5 Ma (Reynolds et al., 2000).

A new pyroclastic event, upper Miocene, was recorded in the Guanaco Formation (Gebhard et al., 1974), the older unit of the Jujuy Subgroup, widely distributed in Lerma, Rio Grande de Jujuy and Juramento-Metán valleys, characterized by alluvial fan and braided fluvial deposits. Distal spessartine-rich garnet -bearing pyroclastic ash-fall deposits distinctive of the Guanaco Formation and identified by Del Papa et al (1993), Viramonte et al. (1994), Tait (2004), Coira et al. (2018) at different profiles: Yacones (*1 Fig. 5) in Lerma Valley, Lumbreras (*12 Fig. 4) and Metán (*10 Fig. 4) in Juramento-Metán Valley, los Alisos (*3 Fig. 5) and Xibi Xibi (*2 Fig. 4) in Río Grande de Jujuy Valley. The nearly identical composition determined in the garnet crystals (Alm70-75Spe21-25Gro1-302 4Pyr0.5-1.) both in the tuff levels and in the proximal facies of the Caldera La Pava-Ramadas (Viramonte et al., 1984; Gauthier et al., 1994; Coira et al., 2018) link the Guanaco Formation tuffs to those in the Ramadas Volcanic Center obsidian and pumice. Moreover $^{40}Ar/^{39}Ar$ ages of the Guanaco Formation tuffs in the Xibi-Xibi profile 6.3 ± 0.3 Ma. $^{40}Ar/^{39}Ar$ ages on glasses (Coira et al., 2018) are within error of the ages, 6.63 ± 0.28 Ma (fission track, Bigazzi, 2004) and K/Ar whole rock of 8,73 ± 0.25 Ma (K/Ar; Viramonte et al., 1994) determined for the Ramadas Volcanic Center and its medial pyroclastic facies.

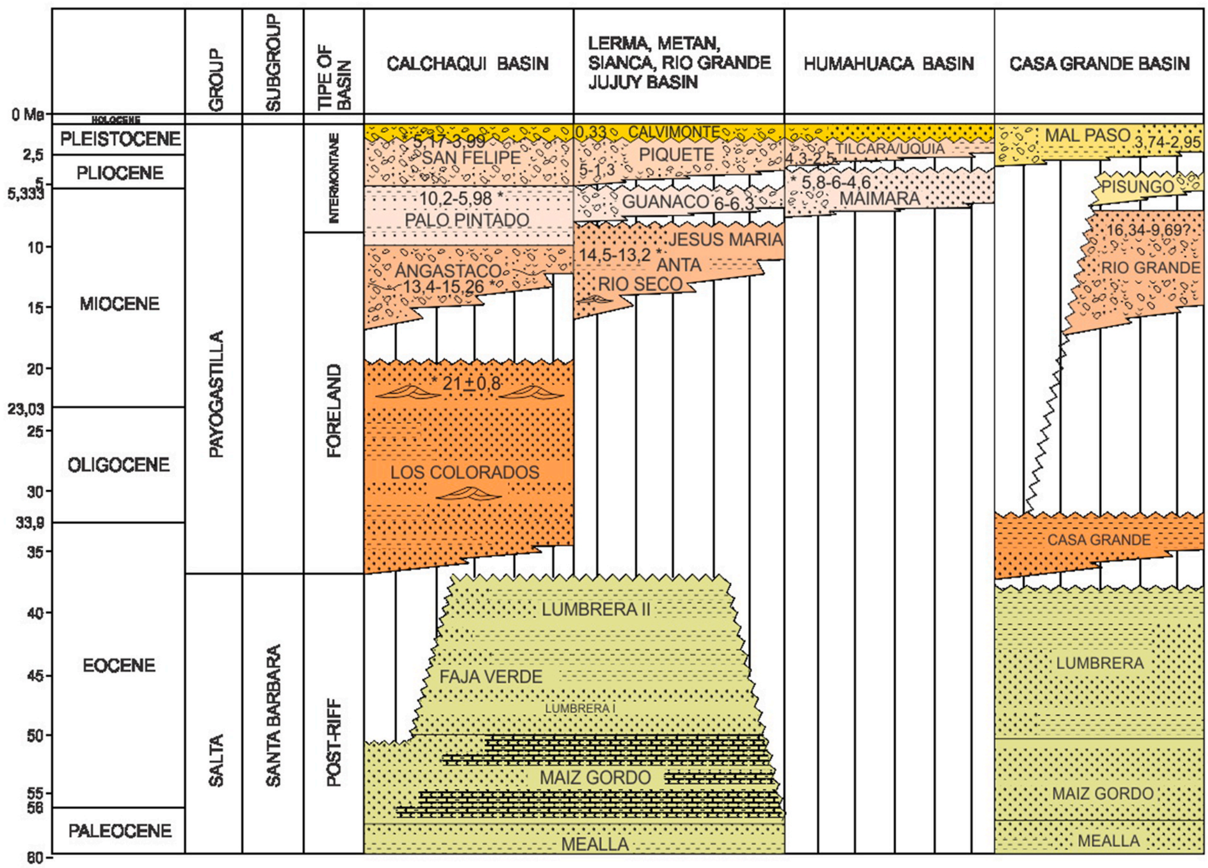

Fig. 3. Lithostratigraphic column of the NW foreland basins.

During the Pliocene two pyroclastic events were recorded in the Piquete Formation, the younger unit of the Jujuy Subgroup, characterized by alluvial fans on the flanks of structural depressions dominated by debris flows and flood plains with small lake systems widespread in the Cordillera Oriental, the Santa Bárbara System, and the Sierra de Zapla (Galli et al., 2017). The first pyroclastic event was registered in the basal section of the Piquete Formation, in Coronel Moldes (*9 Fig. 4, Lerma Valley), where a vitro-crystaline dacitic tuff yielded an age of 5 Ma (fission track in apatite). In the upper third of that unit was recognized in the Arroyo San Vicente section (*8 Fig. 4) , SW of Cabra Corral dam (Lerma Valley) a tuff level of dacitic composition, 25 cm thick, that yielded an age of 1.3 ± 0.2 Ma (fission track dating in apatite, Malamud et al., 1995, 1996). In the overlying Calvimonte Formation (Gallardo, 1985) was identified a tuff level dated at 0.33 ± 0.1 Ma (Malamud et al., 1996).

2.1.3. Humahuaca basin

The Humahuaca Basin is a NNE-oriented intermontane basin in the Eastern Cordillera between the Puna Plateau to the west and the broken foreland of the Santa Bárbara System to the east. It is confined by the fault-bounded Sierra Alta to the west and the Tilcara ranges to the east. During Miocene –Pliocene the synorogenic deposits of the Maimará Formation (Salfity et al., 1984) have accumulated in that fragmented foreland basin (Pingel et al., 2013) and during Pliocene - Pleistocene the Tilcara/Uquía Formations have accumulated in intermountain basins (Streit et al., 2015).

The Maimará Formation is restricted to the central and southern sectors of the Humahuaca basin and their sedimentary facies correspond to an ephemeral fluvial system at the base, developed during an initial stage of accumulation (7–6.4 Ma), a deep braided fluvial system at the middle and to a medial to distal ephemeral fluvial system in the upper sections, along the second stage (6.4–4.8 Ma), as interpreted by Galli et al. (2016). Volcanic ash deposits, rhyodacitic-dacitic in composition are commonly interbedded with the sedimentary clastic successions, mainly among the pro-gradation ephemeral fluvial system facies of the second stage, along the temporal lapse of 5.8–6 Ma to 4.6 Ma. The contribution of these tephras was registered in the Maimará section (Fig. 6) where one of the tuffs yielded an age of 5.8 ± 0.5 Ma (Ar/Ar age, biotite, Galli et al., 2016), similar to a tephra of the basal section of the Huichaira profile (*2 Fig. 6) (5.79 ± 0.19 Ma, U–Pb zircon age, Pingel et al., 2013). Younger tuffs levels (4.6 Ma and 4.8 Ma U–Pb zircon) were recognized in the Incahuasi profile (Pingel et al., 2013) and are correlated with those of the Maimará upper section, for which magnetostratigraphic correlations on the geomagnetic polarity timescale (GPTS) indicate a similar age (4.8 Ma, Galli et al., 2016).

The Uquía Formation (Castellanos, 1950) gather depositional systems as alluvial fans, fluvial (deep sandy gravel-bed braided) and lacustrine/palustrine systems, with frequent intercalations of vitrocrystalline tephras of rhyodacytic-dacitic composition. Two age ranges: 4.3 Ma to 2.6 Ma, were determined among the tephra levels recognized at the different sections along the basin.

The oldest radiometric ages determined in the tuff levels present in the Uquía Formation have been 4.3 to 3.66 Ma in the Incahuasi sector (*1 Figs. 6) and 4.24 to 3.86 Ma in the Quitiacara Sur (*3 Fgig.6) (U–Pb zircon, Pingel et al., 2013), followed by the tuffs of Esquina Blanca South (*6 Fig. 6) with an age of 2.86 Ma (K/Ar age, Marshall et al., 1982). and in the San Roque section (*8 Fig. 6) with a fission track age on zircon at 2.5 Ma (Walther et al., 1998). Within the group of tuffs of younger ages, intercalated in Pleistocene alluvial fans sheet flood deposits, an age U/Pb in zircon was determined to be 2.1 ± 0.02 Ma in a tuff level of the Alonso section (*4 Figs. 6) and 2.21 ± 0,08 in a tuff from Molinos section (*5 Fig. 6) (Streit et al., 2015).

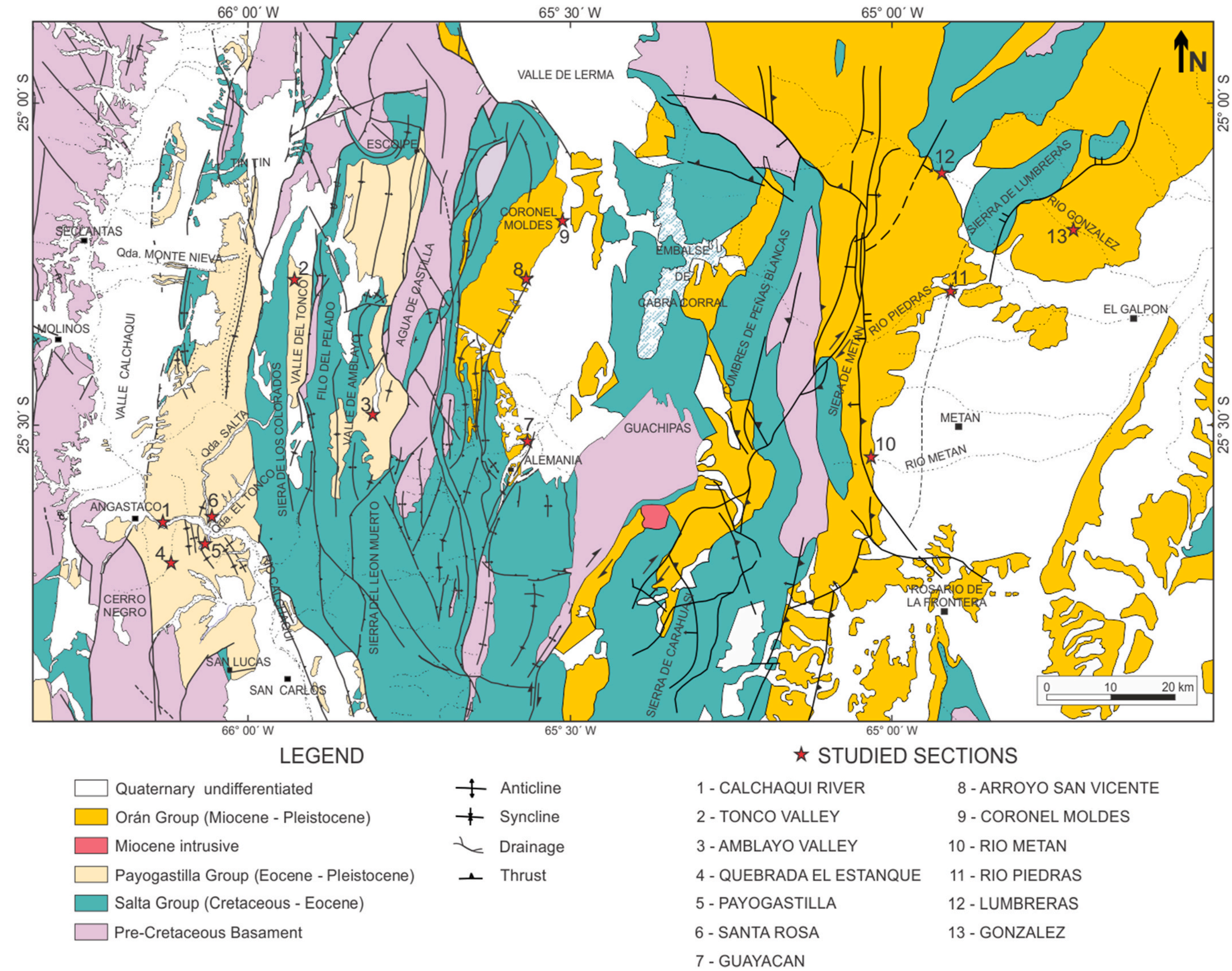

Fig. 4. Geologic map of the Calchaquí, Tonco, Amblayo, Lerma and Metán basins with location of dated tuffs from Payogastilla Group. Modified from Hongn and Seggiaro. 2001; Salfity y Monaldi 2006.

2.1.4. *The Casa Grande basin*

The Casa Grande basin has a complete tecto-sedimentary record of the evolution of the foreland basin system during Eocene-Oligocene and its partitioning into intermontane hinterland basins during Miocene (Siks and Horton, 2011). The sedimentary fill is represented by the Casa Grande formations (Stingl, 1947; Fernández et al., 1973), Río Grande (Pascual et al., 1978), Pisungo (Pascual et al., 1978) and Mal Paso (Fernández et al., 1973; Upper Pliocene - Lower Pleistocene) (Fig. 3.).

Pyroclastic records were recognized in the Casa Grande Basin at tuff levels interspersed in the Mal Paso Formation (temporary equivalent of the Tilcara and Uquía formations in the Humahuaca basin) which yielded Ar/Ar at ages 3.74 to 2.95 Ma (U/Pb zircon, Streit et al., 2015).

3. Ash-fall events and ignimbrite megaeruptions timing along the 21°-26°30′ S

Different ash-fall events were recognized along the basins analyzed across a WE profile: 15-11 Ma; 10–6.8 Ma; 6.4 to 4.8; 4.3 to 2.6; 2.1-Ma-Recent. These ash-fall events mark timelines that allow extending the correlation of the Cenozoic deposits registered across the NW foreland basins (23°-26°S). From the analysis of those events in relation to potential emission sources clearly emerges their agreement with the timing of the ignimbrite flare-up in the region. They show correspondence with the volcanic episodes recognized by Kay et al. (2010) in the northern and the southern Puna, with the pulses recognized by de Silva and Gosnold (2007) and with the stages of eruptions identify by Kern et al. (2016) within the Altiplano - Puna Volcanic Complex (APVC) flare-up.

In a temporal analysis among those Neogene giant calderas of the arc and backarc active at the time of the first ash-fall event are (Fig. 7 a) the Agua Escondida Caldera with the emission of the Ignimbrite Agua Escondida at 13,5 Ma K/Ar (Coira and Kay, 1999) and far in the backarc the Luingo Caldera, with the eruption of the ignimbrites: Alto Lagunas 13.52 ± 0.12 Ma and Pucarilla 12.9 ± 0.3 Ma Ma Ar/Ar, biotite (Guzmán et al., 2011).

In relation to the second event (Fig. 7 a), the Cerro Aguas Calientes Caldera is active at that time with the emission of the Tajamar Ignimbrite: 10.3 ± 0.3 Ma (K/Ar. biotite, Petrinovic et al., 2010), as is the Negra Muerta Volcanic Complex with the emission of the Acay Ignimbrite 9 Ma and Toba I, 7.6 ± 0.3 Ma (Petrinovic et al., 2005) and the Ramadas Volcanic Center with the Corte Blanco Tuff 6.63 ± 0.28 Ma (fission track Tait et al., 2009), and 6.3 ± 0.28 Ma (glass shard Ar- Ar, Coira et al., 2022).

The third event (Fig. 7 b) corresponds with activity at the Guacha Caldera (Guacha Ignimbrite; 5.65 ± 0.01 Ma Ar/A, biotite Salisbury et al., 2011) and at Cerro Galan (Toconquis Group; 5.60–4.68 Ma Ar/Ar, biotite, Folkes et al., 2011).

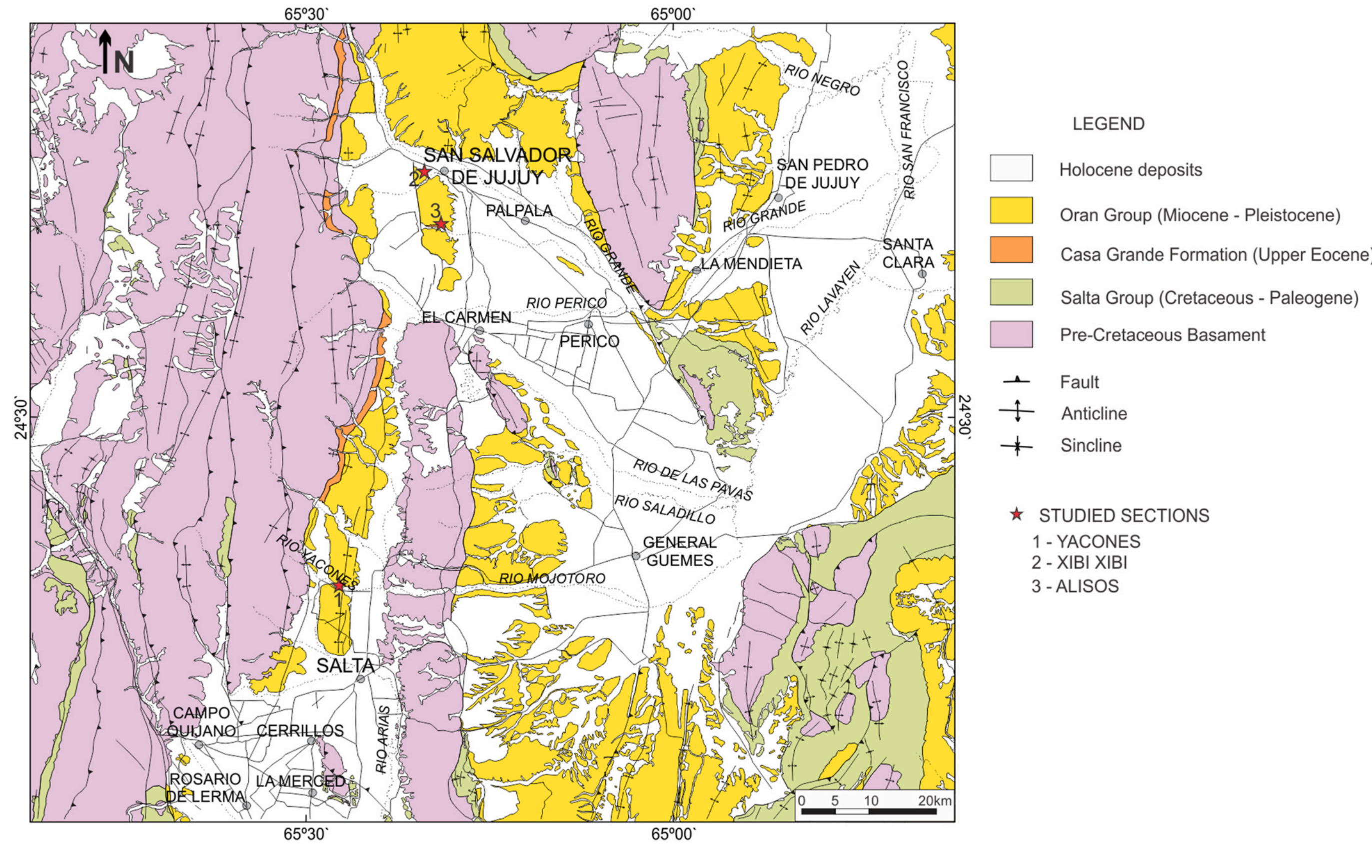

Fig. 5. Geologic map of Río Grande de Jujuy, Sianca, Lerma basins. Modified from R Seggiaro et al. (2019a, b).

The fourth event (Fig. 7 b) corresponds with activity in the Chaxas Complex with the Puripicar Ignimbrite (4.09 ± 0.02 Ma Ar/Ar, biotite, Salisbury et al., 2011), the Pacana caldera with the Atana and Toconao Ignimbrite (3.96 ± 0.02 Ma 4.00 ± 0.012 Ma K–Ar, biotite, respectively, Lindsay et al., 2001), the Guacha Caldera with the Upper Tara Ignimbrite (3.49 ± 0.01Ar/Ar, sanidine, Salisbury et al., 2011), the Laguna Amarga caldera with the Laguna Amarga Ignimbrite (3.8 Ma K/Ar, biotite, Kay et al., 2006 Seggiaro et al., 1999) and the Galan caldera with the Cueva Negra Ignimbrite (3.78 ± 0.08 Ma Ar/Ar, biotite, Folkes et al., 2011).

The fifth event (Fig. 7 b) correspond with the activity of the Purico Complex (Purico Ignimbrite 1.70 ± 0.02 Ar/Ar, biotite), the Guacha Caldera (Puripica Chico Ignimbrite 0.98 ± 0.23 Ar/Ar, biotite), the Laguna Colorada Caldera (Laguna Colorada Ignimbrite 1.98 ± 0.03 Ar/Ar, biotite, Salisbury et al., 2011) and the Cerro Blanco Caldera (Campo Piedra Pómez Ignimbrite 0.44–0.073 Ma 40Ar/39Ar, sanidine/biotite, Viramonte et al., 2008; Cerro Blanco Ignimbrite 0.005 Ma ^{14}C, Montero-López et al., 2010; Fernández-Turiel et al., 2013).

The previous analysis of the ash falls deposits across the different basins in a W-E profile for the same time line have allowed to evaluate their distribution during the different events and to put forward dispersal areas from potential calderas active at that time. consistent with an east-southeast and east-west dispersion from Neogene giant calderas of the arc and the back arc (Fig. 7a and b). as the most distal ashes from Andean eruptions (e.g. Glaze et al., 1989; Scasso et al., 1994; Viramonte et al., 1994; Bailey et al., 2007; de Silva et al., 2009), respectively mainly controlled by northwest and west winds.

4. Ash–fall deposits and ignimbrites from mega-eruptions along the 21°-26°30′ S - textural, mineralogical and depositional characteristics

The representative ash-fall tuffs deposited in the Andean foreland basins in NW Argentina are homogeneous, lack internal structure or normal graded stratified and in some cases reverse graded or laminated (Fig. 8 A; E). These primary deposits are lenticular to laminar in shape with a flat base and show signs of reworking at the upper part of alluvial channel (Fig. 8 B; C). They are associated with layers showing evidence of syn-eruptive re-sedimentation (sense of McPhie et al., 1993) which correspond to units compositionally uniform or showing systematic changes, with structures that indicate rapid deposition (combination of mass flow, hyperconcentrated flow or traction currents) with dominance of juvenile ash clasts, texturally unmodified, and scarcity or absence of lithics and homogeneity in their phenocrystals (Fig. 8 C). These banks are usually associated with levels showing evidence of rework post-eruptive and re-sedimentation with consequent sedimentary mixing which often have irregular geometries, and show internal bedding (Fig. 8 F), some displaying meter-sized channels or present multiple ash layers interfinger with alluvial sediments.

The host sedimentary sequence consists, depending on the location within the basins and their evolution of: sand-gravel braided fluvial system associated with gravity flows, alluvial fan systems debris flow dominate, flood plains, sheet flood deposits and ephemeral lakes.

The textural and petrographic characteristics that characterize the average of the studied tuffs deposits in the basins under consideration, correspond to tuffs that are predominantly rich in crystals (20–30%), although vitreous tuffs (1–5% crystals) are also represented. They have vitroclastic textures, showing bubble-wall glass shards with cuspate or tubular shapes and variable content in pumice fragments, all of them immersed into a fine vitreous mesostasis. Blocky glass shards are infrequent.

The crystal richness observed in the studied tuffs could be reflecting crystals rich, dense, sluggish and poorly inflated nature of the ignimbrite sources, which retarded elutriation of ash to feed large co-ignimbrite ash clouds (Ort, 1993; de Silva et al., 2006; Folkes et al., 2011). Although ash elutriation happens it is not thought to have been efficient with a

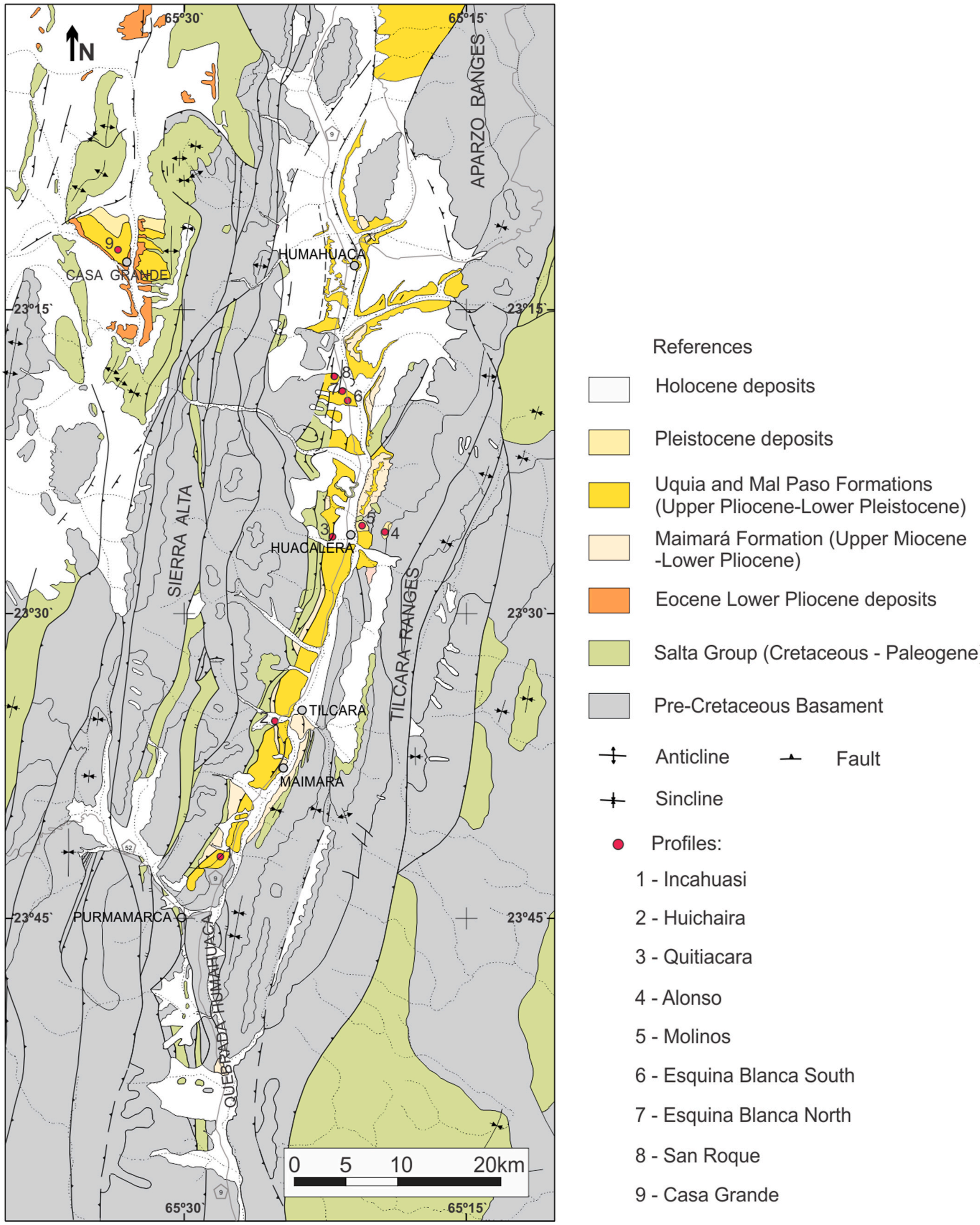

Fig. 6. Geologic Map from Humahuaca –Casa Grande basins. Modified from González et al. (2003).

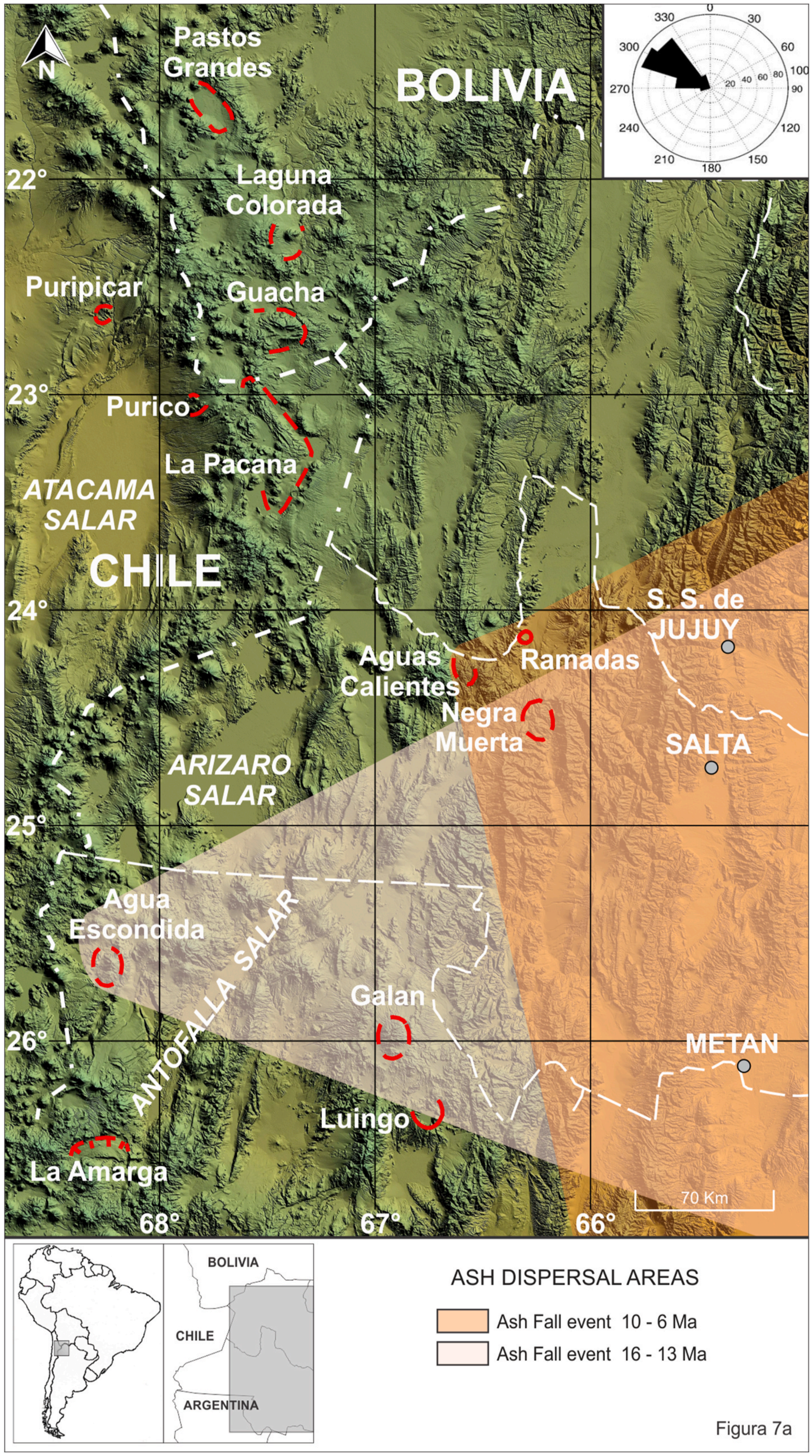

Pastos Grandes
BOLIVIA
Laguna Colorada
Puripicar
Guacha
Purico
La Pacana
ATACAMA SALAR
CHILE
Aguas Calientes
Ramadas
S. S. de JUJUY
Negra Muerta
SALTA
ARIZARO SALAR
Agua Escondida
ANTOFALLA SALAR
Galan
METAN
Luingo
La Amarga
70 Km
22°
23°
24°
25°
26°
68°
67°
66°
N
BOLIVIA
CHILE
ARGENTINA
ASH DISPERSAL AREAS
Ash Fall event 10 - 6 Ma
Ash Fall event 16 - 13 Ma
Figura 7a

Fig. 7. 7a; y 7 b. Satellite Radar Topography Mission (SRTM) image of the Central Andean plateau showing the Cenozoic Giant Calderas with discrimination of ash fall tuff events and dispersion areas. Insert is with directions rose determined around APVC calderas based in erosional structures (after Greene, 1995; Bailey et al., 2007).

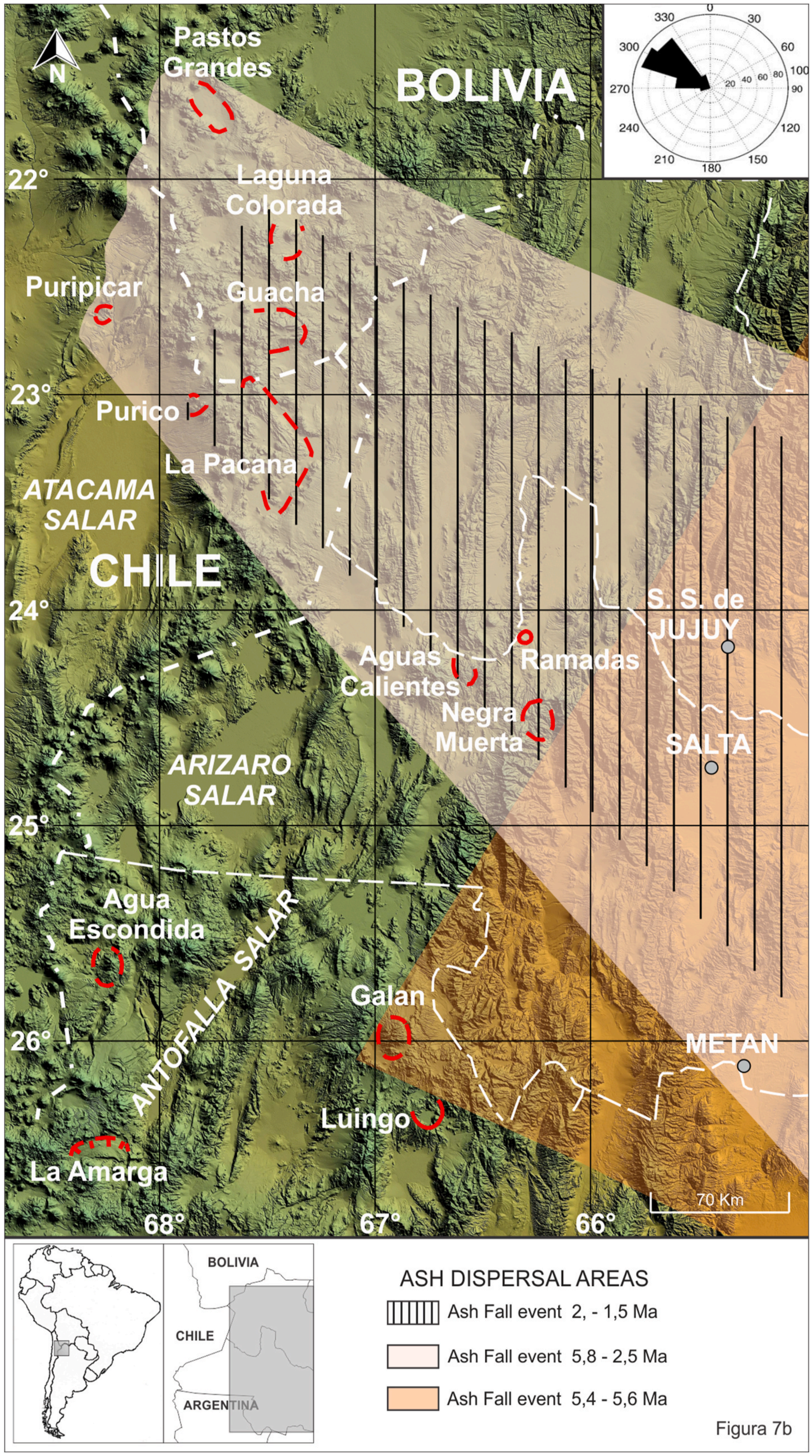

Fig. 7. (*continued*).

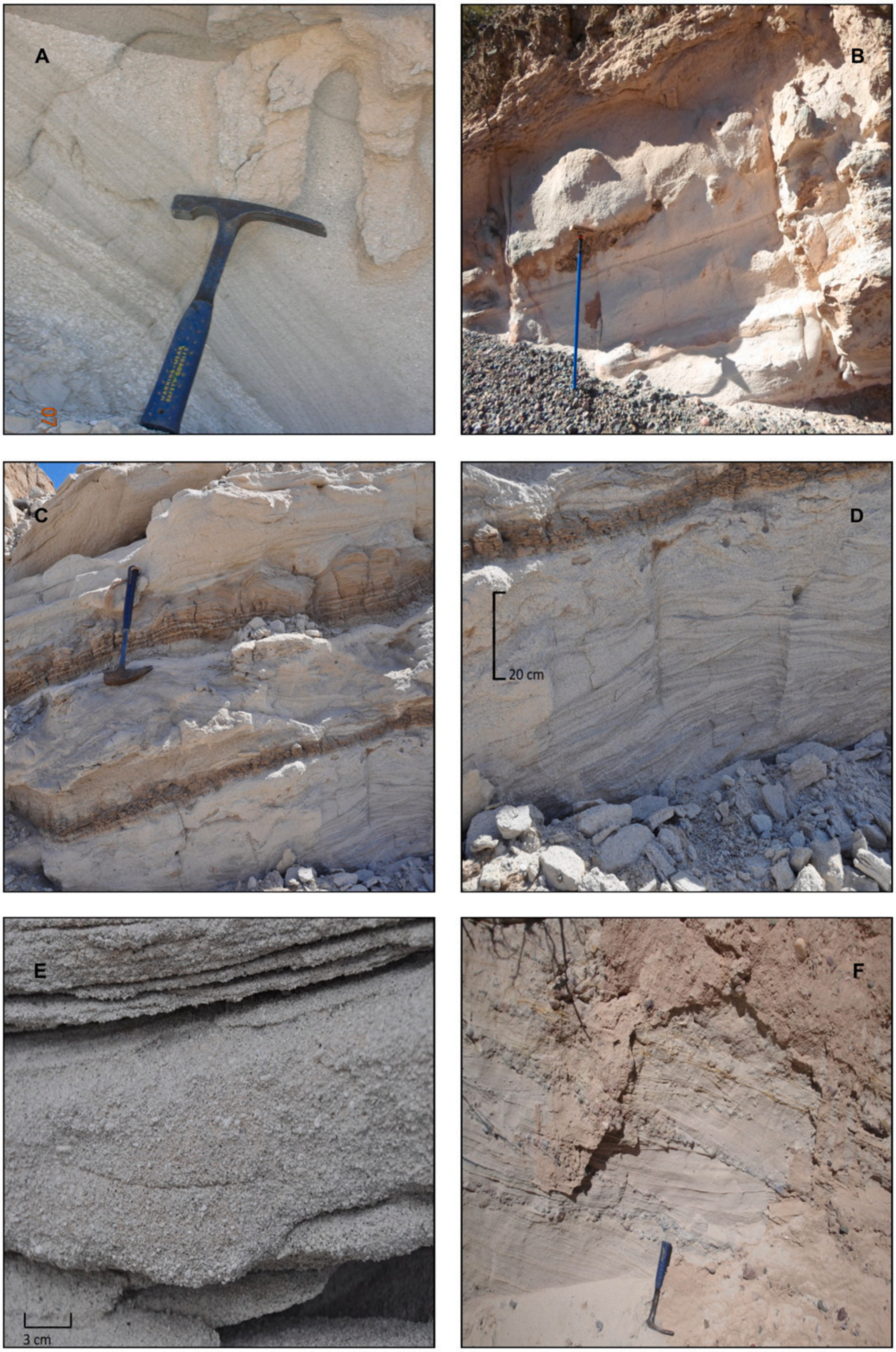

Fig. 8. An Ash-fall tuffs of the Palo Pintado Formation massive to finely laminated, towards the base rich in pumice. Qda El Estanque profile (4 in Fig. 4); **B** Massive ash-fall tuffs of the Maimará Formation reworked on the roof. Incahuasi profile (1 in Fig. 6); **C** Upper ash-fall tuff layer massive to slightly laminated of the San Felipe Formation. filling a channel made in an underlying siltstone bank. Intermediate resedimented (syneruptive) ash fall deposit with structures that indicate rapid deposition. Rio Calchaquí. profile1 in Fig. 4; **D** Bank of resedimented tuff with cross stratification from the base of the previous profile shown in C.; **E** Coarse ash-fall tuff rich in pumice. On top laminated from San Felipe Formation. Qda Payogastilla (5 in Fig. 4); F Secondary ash-rich deposits of the Uquía Formation with scarce clasts of Pre cenozoic basement rocks indicating sedimentary mixing, Esquina Blanca South profile (6 in Fig. 6).

crystal enrichment factors of 17–47%(de Silva and Francis, 1989; Folkes et al., 2011).

To this should be added not easy distinction between primary ash fall depositis from those that represents syn-eruptive resedimented deposits (McPhie et al., 1993).

Their mineralogy has shown few variations, its essential components are andesine to oligo-andesine, quartz, biotite and hornblende and as accessories pyroxene, magnetite, zircon and minor titanite. Hornblende only is accessory in some cases (e.g. Maimará-San Felipe formations).

The voluminous ignimbrites (>500 up 2200 km^3, DRE) erupted from those large, multicyclic calderas along the 21°-26°30′ S, are massive, show few segregation structures, lack of Plinian fall deposits and generally shared similar petrographic characteristics and show correspondence with the ash-fall tuffs here considered. They are crystal rich with coarse crystal fragments of plagioclase, quartz, biotite, amphibole, Fe–Ti oxides, and occasional sanidine in the more silicic (>69% SiO_2)

along with ubiquitous pyroxene, apatite, titanite and zircon.

5. Correlations of ash-fall tuffs across the Andean foreland basins and analysis of their link to the Neogene ignimbrite flare-up

Mineralogical and geochemical data of ash-fall deposits were analyzed for each event in order to characterize them during the different pulses recorded across the foreland basins. Those data were analyzed in contrast with those of the contemporary ignimbrites of the Neogene ignimbrite flare up (Table 1) to test the feasibility to identify their potential sources.

The first Neogene volcanic event (16-11 Ma) to be considered had a wide diffusion and record particularly in the Calchaquí, Tonco, Amblayo, Lerma, Metán and Sianca intermountain basins, represented by significant deposits of ash fall-tuffs. Such a magmatic event registered in the segment 25°-27° S was associated with a period of shallowing of the subducting slab, as Juan Fernandez ridge was subducting (Kay and Coira, 2009), that explains the eastward broadening of arc magmatism represented by long-lived stratovolcanoes and ignimbrite eruptions that extended eastward in the arc as for example Agua Escondida caldera (13, 5 Ma, Coira et al., 2022) and far into the back arc at the 14.5–11.5 Ma Luingo (Guzmán et al., 2011).

On geochronological, mineralogical and geochemical data were postulate as possible sources of those ash-fall tuffs recorded in the cited intermountain basins: Agua Escondida caldera or the eastern Luingo caldera. The geochemical characteristics of the Agua Escondida Ignimbrite, from homonymous caldera and the Alto de las Lagunas Ignimbrite from Luingo caldera show correlation with those of Angastaco Formation ash fall tuffs (Fig. 9 a, b, c) which exhibit discriminating trace element ratios of Sm/Yb = 1,6–2,4, that reveal residual clinopyroxene in the magma source region, La/Ta = 11–32 that supports a role for an underlying slab and Th/La = 0.2–0.5 that indicate moderate cortical contamination. The discriminating trace element ratios of the Agua Escondida Ignimbrite are Sm/Yb = 2.16–2,8 La/Ta = 20,8–23, Th/La = 0,2–0,3 (Coira y Kay 1999) and those of the Alto de las Lagunas are: Sm/Yb = 2,09–2,8, La/Ta = 24–35, Th/La = 0,5. (Guzmán et al., 2011).

In the lapse 10-6 Ma are recorded ash-fall tuffs in the Palo Pintado Formation which begins its accumulation in the Calchaquí basin from 10 to 6 Ma. At 8–6.6 Ma in the Lerma, Metán, Río Grande de Jujuy basins singular ash fall tuffs garnet bearing are recognized in the Guanaco Formation.

During that lapse of time took place tectonic reactivations, that caused an increase in A/S rate, also associated with a change in the

Table 1
Mineralogical a geochemical characteristics of the tuffs in comparison with those of coeval ignimbrites of APVC and southern Puna calderas.

Ignimbrite	Source caldera	Eruption age Ma ±2δ *	Minerals	% SiO2	Geochemical ratios	References
Purico	Purico	0.98 ± 0.23	Pl,Hbl,Qtz,Bt,Opx,Mag	65–70%	La/Yb12-18,Sm/Yb2.3-3,La/Sm5.5-6, La/Ta20-32	de Silva 1991 Schmitt et al., 2001
Puripica Chico	Guacha	1.70 ± 0.02	Pl,Qtz,Bt,Hbl,Mag,Ap	67%	La/Yb15-21,Sm/Yb3-3.3,La/Sm5.2–6.5,La/Ta26-33	Salisbury et al. (2011)
Lg. Colorada	Lg. Colorada	1.98 ± 0.03	Pl,Qtz,Bt,Mag,Ilm	64%	La/Yb18,Sm/Yb3.5,La/Sm5.5,La/Ta25	Salisbury et al. (2011)
Tara	Guacha	3.49 ± 0.01	Pl,Hbl,Bt,Cpx,Mag	68–70%	La/Yb10-20,Sm/Yb2.5–3.7,La/Sm4-6.1,La/Ta12-31	Salisbury et al. (2011)
Atana	La Pacana	3.96 ± 0.02	Pl,Qtz,Bt,Hbl,Mag,Opx, Cpx,Ilm	60–72%	La/Yb13-18,Sm/Yb2.5–3,La/Sm4.5–6.5,La/Ta12-31	Kay et al. (1999) Lindsay et al. (2001)
Toconao	La Pacana	4.00 ± 0.012	Pl,Qtz,Bt,Sa	73–74%	La/Yb9-11,Sm/Yb1.9–2,La/Sm4.5–5.8,La/Ta10-12	Kay et al., 1999 Lindsay et al. (2001)
Puripicar	Chaxas	4.09 ± 0.02	Pl,Qtz,Bt,Hbl,Mag	67%	La/Yb20-21,Sm/Yb3.2–3.9,La/Sm5.6–6.1,La/Ta30	de Silva 1991
Merihuaca	Galan	5.5–6.4	Pl,Qtz,Bt,Hbl,Mag Ap Zrn	69–69.6%	La/Yb21-36,Sm/Yb5.5-6,La/Sm5-6, La/Ta19-24	Kay et al. (2010)
Guanaco Fm.tuffs	Ramadas Volcanic Complex	6.63	Grt,Sa,Qtz,Mag,Mnz	70–75%	La/Yb6-10,Sm/Yb3-4.2,La/Sm8-10, La/Ta3-4	Coira et al. (2018)
Toba I	Negra Muerta	7.6	Pl,Qtz,Bt,Sa,Ap,Zrn,Mag	71–72%	La/Yb20-25,Sm/Yb3.9,La/Sm4-6,La/Ta23	Petrinovic et al., 2005
Tajamar	Aguas Calientes	10.3	Pl,Qtz,Bt,Cpx,Mag,Zrn	64–66%	La/Yb21-25,Sm/Yb3-3.7,La/Sm6.3–6.7,La/Ta23-36	Petrinovic et al., 1999
Alto de las Lagunas	Luingo	13.52	Pl,Qtz,Bt,Hbl,<Sa,Mag, Ap,Zr.Ttn	65–66%	La/Yb10-15,Sm/Yb2-2.8,La/Sm6.4.8–5.6,La/Ta24-35	Guzman et al., 2011
Agua Escondida	Agua Escondida	13.5	Pl,Qtz,Bt,Hbl,<Cpx,Mag Ap Zrn	63–64%	La/Yb7-19,Sm/Yb2-2.8,La/Sm5-6.2, La/Ta20-24	Coira and Kay, 1999
Angastaco Fm. ash-fall tuffs		13.4–15.3	Pl,Qtz,Bt,Hbl,<Cpx,Mag Ap Zrn,Ttn	70-65%	La/Yb10-11,Sm/Yb1.6–2.4,La/Sm4-6.2,La/Ta11-32	Coira et al. (2014)
Palo Pintado Fm.ash-fall tuffs		10.2–5.98	Pl,Qtz,Bt,Hbl,<Cpx,Mag Ap Zrn,<Ttn	63–64%	La/Yb18-22,Sm/Yb3.9–4.1,La/Sm4.2–5.3,La/Ta21-24	Coira et al. (2014)
San Felipe Fm ash-fall tuffs		5.17–3.99	Pl,Qtz,Bt,<Hbl,Mag Ap Zrn,Ttn	64–65%	La/Yb22-25,Sm/Yb4-5.6,La/Sm5.5–6.2,La/Ta19-35	Coira et al. (2014)
Maimara Fm ash-fall tuffs		4.6–6	Pl,Qtz,Bt,<Hbl,Mag Ap Zrn,Ttn	67–72%	La/Yb31-33,Sm/Yb4.5–5.3,La/Sm6-7, La/Ta22-28 La/Yb10-20,Sm/Yb2-2.8,La/Sm6-7, La/Ta10-20	Galli et al. (2016)
Uquia-Mal Paso ash-fall tuffs		2.6–4.3	Pl,Qtz,Bt,Hbl,<Px,Mag, Zrn	58–70%	La/Yb10.20,Sm/Yb2.1–3.2,La/Sm5.3–8.5, La/Ta12-33	Coira et al., 2022
Pleistocene ash-fall tuffs		2.1–1	Pl,Qtz,Bt,Hbl,Cpx,Opx Mag,Zrn	61–69%	La/Yb11-25,Sm/Yb2.3–4.1,La/Sm4.2-8,La/Ta22-40	Coira et al., 2022

Abbreviations for names of rock-forming minerals (Whitney,D.L.and Evans,B.W.2010).

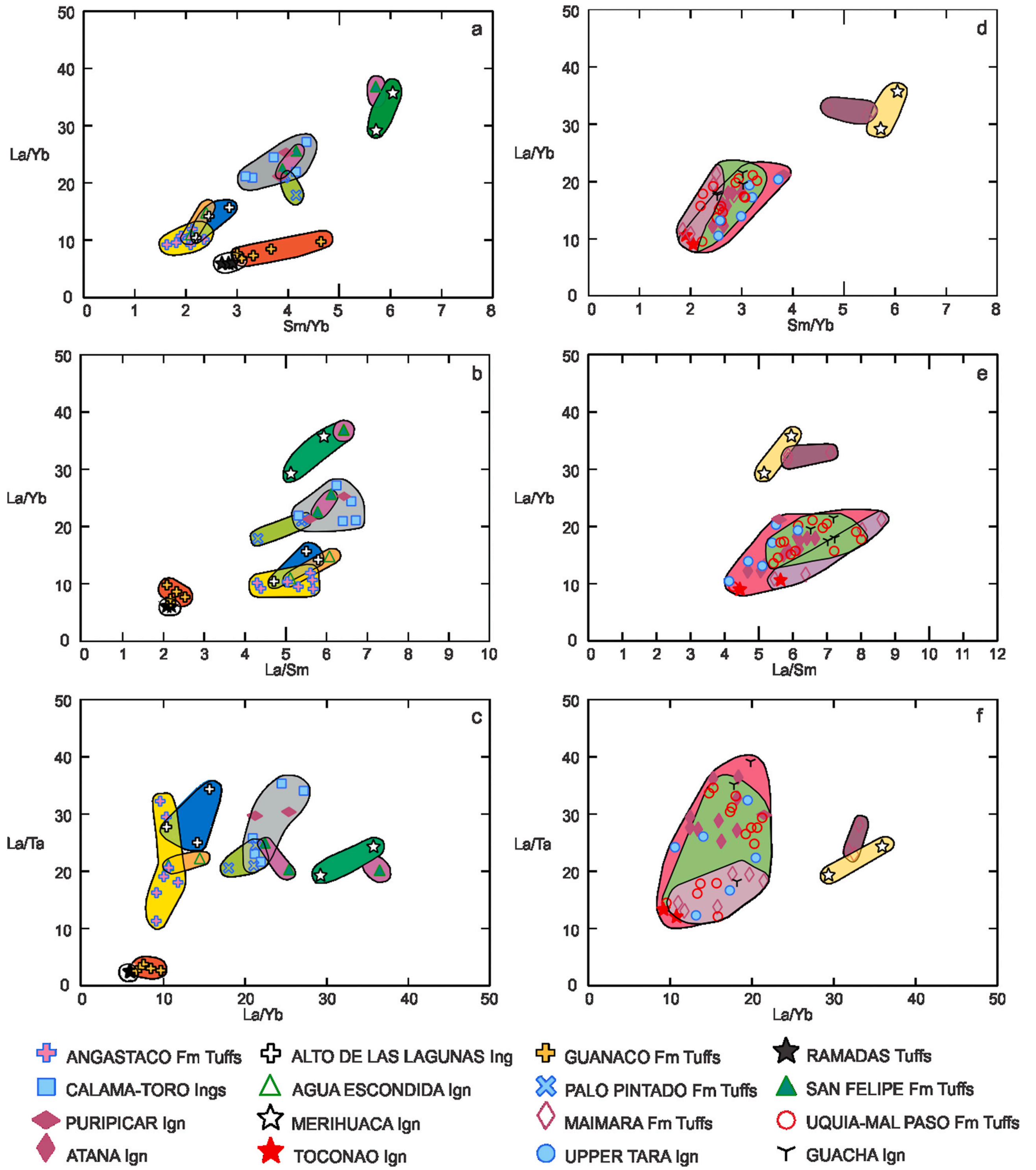

Fig. 9. Plots of trace element ratios showing in 9 a, b, c fields color labeled for: Angastaco (yellow), Palo Pintado (light green), Guanaco (light rose) and San Felipe (violet) formations tuffs and for comparison Agua Escondida (orange), Alto Lagunas (light blue), Calama –Toro- Puripicar (grey), Merihuaca (green) ignimbrites, Ramadas tuff (uncolored). In 9 d, e, f showing figures fields color labeled for: Maimará (violet), Uquía and Mal Paso (green) formations tuffs and for comparison APVC ignimbrites (rose): Guacha, Atana, Toconao, upper Tara ignimbrites field.

petrological composition of its deposits as pointed by Galli et al. (2011) and the formation of orographic barriers that determined more warm and humid conditions in the basins (Starck and Vergani, 2001; Starck and Anzotegui, 2001).

The ash-fall tuff deposits of Palo Pintado Formation present geochemical characteristics as: significant enrichment in HREE (Sm/Yb = 3,9–4,1) in relation to tuffs from the 16-11 Ma volcanic l event (Sm/Yb = 1,6–2,4) and La/Ta = 21–21.2, Th/La = 0,5–0,6 similar to those of volcanic centers of the Calama-Olacapato-El Toro System active by 10–7 Ma, such as the Caldera Cerro Aguas Calientes and its Ignimbrite Tajamar (Fig. 9 a, b, c) Sm/Yb = 3,0–4,3 La/Ta = 21,7–34,5 Th/La = 0,3–0,4 (Petrinovic et al., 1999) and the Complejo Volcánico Negra Muerta: Toba I Sm/Yb = 3,9, La/Ta = 23, Th/La = 0,3–0,4 (Petrinovic et al., 2005).

The rhyolitic ash fall tuff deposits of Guanaco Formation are distinctive in having euhedral spessartine almandine garnets as their only phenocryst, as well as geochemical features consistent with Ramadas Volcanic Center rhyolitic tuffs characterized by a distinctive strongly peraluminous Mn-rich garnet-bearing (Viramonte et al., 1994; Tait, 2004: Coira et al., 2018) Sm/Yb ratios ~3.0–4.2 that require heavy REE retention in residual hornblende and garnet in the source, very low La/Ta = 3–4 and Th/La = 0.7–0.85 (Fig. 9 a, b, c).

A new volcanic pulse (5-4 Ma) was recorded in the Calchaquí basin as tuff deposits accumulated in the San Felipe Formation. At~5 Ma, the Angastaco basin would have possibly been separated from the rest of the Cenozoic foreland basin, with partial connections of first and second order rivers that would have drained to the east (Galli et al., 2014). The ash fall tuffs of San Felipe Formation show, as observed in the case of tuffs of the Palo Pintado Formation, enrichment in HREE (Sm/Yb = 4–5.6), for similar content in LREE (La/Sm = 4–6.2), in relation to those of the Angastaco Formation (Sm/Yb = 1.6–2.4), reflecting the presence of residual hornblende to garnet instead of clinopyroxene in the magma source region of the last one, consistent with evolutions at increasing depths. Both show moderate arc filiation (La/Ta = 20–31). The tuffs of San Felipe Formation from basal to middle sections show mineralogical and geochemical characteristics similar to the ignimbrites of the Toconquis Group (Merihuaca Ignimbrite) erupted from the Cerro Galan Caldera in southern Puna (Coira et al., 2014) and in the upper sections to Puripicar Ignimbrite from Puripicar caldera of the Altiplano–Puna Volcanic Complex at 300 km al NW of the Calchaquí Valley. During the 6-3 Ma lapse occurred in the Southern Puna a notable eastward frontal arc migration, developed of intraplateau basins bounded by high ranges, and were erupted voluminous 6-2 Ma ignimbrites, and 7-0 Ma back arc mafic flows. That evolution was modeled by a moderately shallow slab producing widespread volcanism with subsequent steepening by 6 Ma leading to delamination of dense lithosphere culminating in the eruption of the voluminous Cerro Galán ignimbrite at 2 Ma (Kay et al., 1999; Kay and Coira, 2009). Meanwhile at that time in Northern Puna further steepenig of slab give place to migration of large ignimbrite centers to the arc region (APVC) in coincidence with the change to an out-of-sequence thrusting in the Subandean belt near 4.4 Ma.

In a wide area that included the Eastern Cordillera, Santa Bárbara System and Sierra de Zapla, ash fall deposits, link to the Pliocene volcanic pulse (5-3 Ma), were recorded in the Piquete Formation (5–1.3 Ma). The deposits of the Piquete Formation were accumulated as a consequence of the strong structuring produced by the uplift of the Sub-Andean belt the Santa Bárbara System and part of the Eastern Cordillera, with the formation of intermountain basins, such as the Lerma Valley and the Siancas Valley. These tuffs are characterized by enrichment in HREE (Sm/Yb = 3.8–4.2, indicative of residual hornblende in the magma source region), high La/Sm = 7–9 and moderate arc filiation La/Ta = 20–23 (Fig. 9 d, e, f).

In the Quebrada de Humahuaca this volcanic pulse was recognized in the tuffs deposit of the Maimará Formation (6.4–4.8 Ma Ma). The syn-orogenic deposits of the Maimará Formation (Upper Miocene - Lower Pliocene) have accumulated in a fragmented foreland basin (Pingel et al., 2013). Based on the geochemical characteristics of the Maimará Formation tuffs two volcanic inputs are recognized during the sedimentation of Maimará Formation. The REE characteristics of these ash fall tuffs in two groups representative of those input (Fig. 9 d, e, f). The first group includes the samples from the middle Maimará section which exhibit moderate LREE enrichment (La/Sm = 5–8) and low Sm/Yb ratios (2–3), that require residual hornblende. The second group includes the samples from the lower part of the Maimará section with La/Sm = ~5.3–8.5 are similar to those of the group 1 and higher Sm/Yb = ~4.5–5.4 requiring instead residual garnet, consistent with a higher pressure residual mineral assemblage at depth. The ash deposits of the first group are chemically most like the ignimbrites originated from the Guacha and Pacana calderas enrichment (La/Sm = 5–7) and low Sm/Yb ratios (2.2–3.5), active at that time located 200–230 km west of the study region.

In contrast, the second group shows geochemical affinities with the contemporaneous Merihuaca Ignimbrite from the Galan caldera located 290 km south-southwest (Galli et al., 2016) with high Sm/Yb = 5.2–5.8, La/Sm = 5.2–6.3.

During 4.3 to 2.6 Ma in the Quebrada de Humahuaca and Casa Grande intermountain basins the volcanic pulse was recognized in the tuff deposits of the Uquía and Mal Paso formations and at 2.1–2.2 Ma another volcanic pulse was recorded in Pleistocene alluvial fans sheet flood deposits.

The tuffs of both groups are mainly of a rhyodacite-dacite composition with minor component of andesites to trachyandesites and can be classified as peraluminous, bordering meta-aluminous (A/CNK = 1.05–1.39). They are characterized by 58–69% SiO_2 anhydrous contents, similar Na_2O (1.1–4.5%), K_2O (1.1–4.8%) and TiO_2 contents (0.2–0.8%.), with FeO/MgO (0.8–2.8) and plot in the calc-alkaline range and with the highest values in the tuffs recorded in Pleistocene alluvial fans sheet flood deposits. The major difference between the two groups lies in trace elements with the REE diagram patterns denoting a slight enrichment in LREE in the younger tuffs in relation to those in Uquía and Mal Paso formations (La/Sm ratios~4.5–8.2 vs 4.0–7.2) with similar Sm/Yb ~2.1–4.2. and an increased arc affiliation in the younger tuff group (La/Ta 22–44 vs 12–32). The La/Yb and Sm/Yb in both groups of tuffs indicate sequestration of HREE in residual hornblende with the highest ratios in the tuffs intercalated in Pleistocene alluvial fans sheet flood deposits (Fig. 10).

Detailed comparison of integrated petrographic, geochemical, and geochronological data with ignimbrites erupted from regional Plio-Pleistocene calderas (Table 1), lead us to postulate that the Pliocene tuffs from the Uquía and Mal Paso formations were likely sourced from La Pacana caldera (Atana and Toconao ignimbrites), the Guacha Caldera (Tara Ignimbrite), and/or the Puripicar caldera (Puripicar Ignimbrite). The mainly Pleistocene tuffs intercalated in alluvial fans sheet flood deposits, on the other hand, appear to have been sourced from the Purico Complex (Purico ignimbrite), the Guacha Caldera (Puripica Chico ignimbrite), and/or the Laguna Colorada Caldera (Laguna Colorada Ignimbrite).

The temporal, mineralogical and geochemical correlations observed among the ash-fall tuffs deposited across the Andean foreland basins and APVC ignimbrites, the southern.

Puna large caldera and the volcanic centers of the Calama-Olacapato-El Toro System highlight “the distinctive signature” of those megacalderas systems which facilitates such correlation. That signature is in accordance with the recognition of the “regional geochemical trends” of the Andean ignimbrites according location and time, as has been indicated in previous studies (Kay et al., 1988; Kay and Coira, 2009; Kay et al., 2010; Mamani et al., 2010, Brandmeier and Wörner, 2016 and references therein) characteristics linked to basement differences, along with temporal changes in that basement, thermal and structural evolution of the crust, distinct regimes of partial crustal melting and mantle melt compositions, evolved over a changing variable steepening subduction zone (de Silva, 1989; Coira et al., 1993; Ort et al., 1996; Kay et al., 1994, 1999; Lucassen et al., 2000; Lindsay et al., 2001; Zandt et al., 2003; Sobolev et al., 2005; Trumbull et al., 2006; de Silva and Gosnold, 2007; Schnurr et al., 2007; Kay and Coira, 2008, 2009; Kay et al., 2010, 2011; Folkes et al., 2011; Guzmán et al., 2014 and references therein).

6. Concluding remarks

The stratigraphic, textural, petrographic, geochemical and geochronological characteristics of ash-fall deposits preserved in Andean foreland basins Neogene deposits across the region from 23°-26°S show these ash-fall tuffs as excellent chrono-stratigraphic tracers of tecto-sedimentary events across the basins, as well as keys to identify their potential magmatic sources.

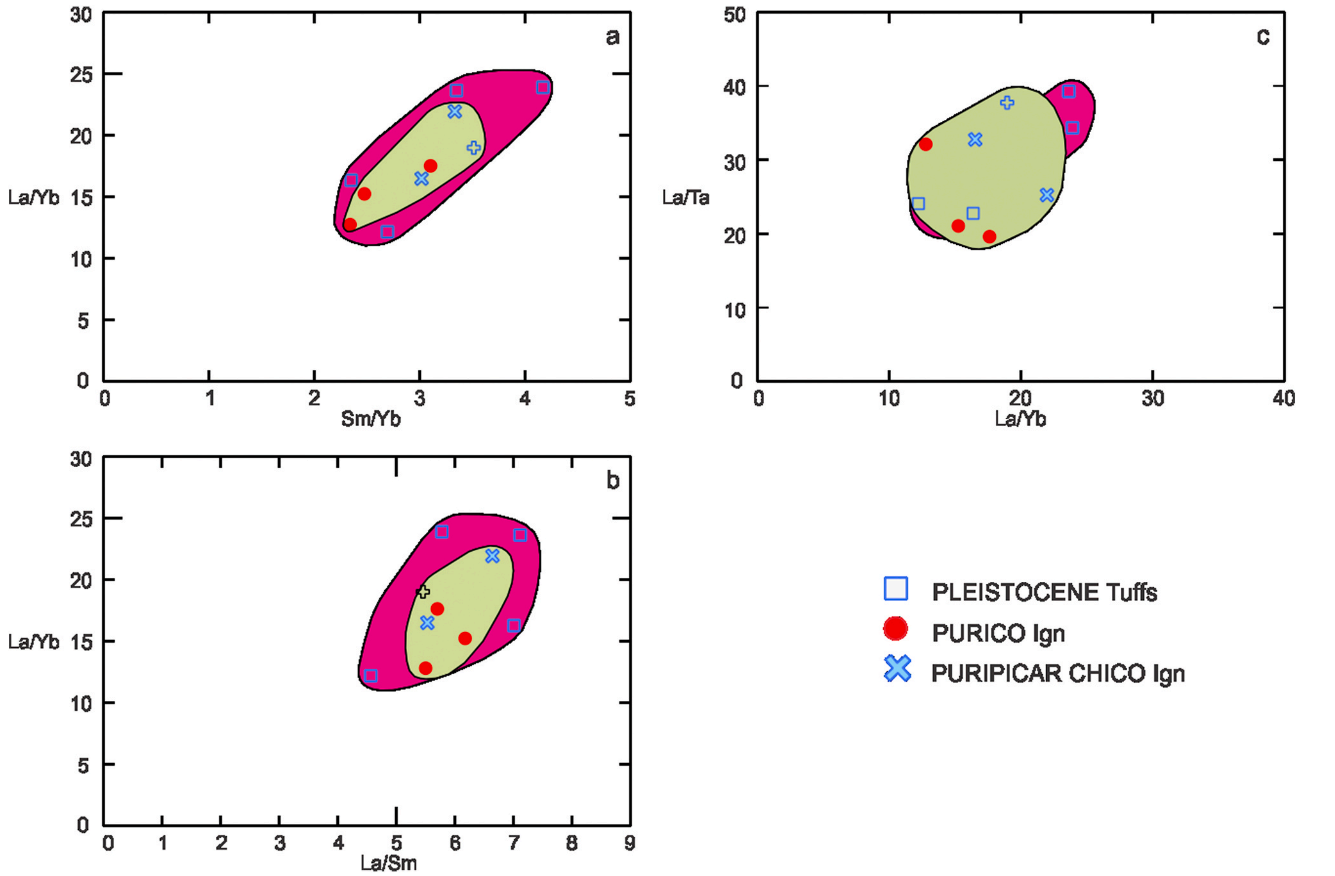

Fig. 10. Plots of trace element ratios showing fields color labeled of Pleistocene tuffs (rose) in comparison with those of Purico and Puripicar Chico ignimbrites (light green).

Different ash-fall events were recognized along the basins analyzed across a WE profile: 15-11 Ma; 10–6.8 Ma; 6.4–4.8; 4.3–2.6 and 2.1-Ma-Recent. These ash-fall events mark time lines that extend the correlation of the Cenozoic deposits registered across the NW foreland basins (23°-26°S).

The ash-fall tuffs events are concordant with the timing of the ignimbrite flare-up in the region.

Detailed comparison of integrated petrographic, geochemical, and geo-chronological data of the studied ash-fall tuffs with ignimbrites erupted from Altiplano–Puna Volcanic Complex and southern Puna calderas have made it possible to identify their emission centers. Thus the ash-fall tuffs of the first event, recorded from the Calchaquí basin to the Metán basin were likely sourced from back arc calderas like Agua Escondida and Luingo. In the lapse 10-6 Ma the Cerro Aguas Calientes Caldera, the Complejo Volcánico Negra Muerta and the Ramadas Volcanic Center appear to be the emission centers of the ash fall deposits in those basins. At 5-4 Ma volcanic pulse the Puripicar caldera from the APVC and Galán Caldera from southern Puna were postulated as the emission centers. In the Quebrada de Humahuaca and Casa Grande basins the ash-fall tuffs deposited during the lapse 6.4–0.8 Ma show characteristics that point to a dominant contribution of APVC centers like Pacana, Guacha, Puripicar calderas with a meager contribution from the Galan caldera.

The analysis of the distribution of the ash-fall deposits across the different basins in a W-E profile for the same timeline in relation to the location of the potential emission calderas active at those times has allowed to conclude that their distribution is consistent with an east-southeast, and in minor scale, east northeast dispersion from Neogene giant calderas of the arc and the back arc respectively controlled by northwest, west and south winds.

The results highlight the importance that the ash-fall deposits reach to achieve a regional chrono-stratigraphy of the foreland basins in the Andean margin between 23°-26° S during Cenozoic times, to identify their link to the Andean Neogene ignimbrite flare-up and to delineate their dispersion patterns.

CRediT authorship contribution statement

Beatriz Coira: Investigation. **Claudia I. Galli:** Investigation. **Suzanne Mahlburg Kay:** Investigation. **Ricardo N. Alonso:** Investigation. **Patrocinio Flores:** Formal analysis. **Edgardo David González:** Software.

Declaration of competing interest

The authors declare that they have no known competing financial interests or personal relationships that could have appeared to influence the work reported in this paper.

Acknowledgments

This research was funded by the AGENCIA (PICT-2017-1010), PUE-INECOA (22920170100027CO), CI-UNSa 2013–2287 and SECTER-UNJu 08/E036-E0035.

We thank Alejandro Perez for his invaluable collaboration in the field survey and sample processing, as well as for his constructive and positive suggestions, Roberto Liquin and Paulino Cachizumba for their support in laboratory work.

References

Arias, J.E., Chávez Manrique, A., 1976. El Grupo Orán en el Valle de Lerma. Salta, 424 Rev. Asoc. Geol. Argentina 31 (1), 5 9–6 0.

Bailey, J.E., Self, S., Wooller, L.K., Mouginis-Mark, P.J., 2007. Discrimination of fluvial and eolian features on large ignimbrite sheets around La Pacana Caldera, Chile, using Landsat and SRTM-derived DEM. Rem. Sens. Environ. 108 (1), 24–41.

Bigazzi, G., 2004. Fission track dating of the Corte Blanco tuff. In: Tait, M.A. (Ed.), Dynamics Eruption Dynamics and Evolution of a Highly Explosive Rhyolitic Volcanic Complex in the High Andes: the Late Miocene Ramadas Volcanic Centre, Andean Puna, Salta Argentina. Ph.D. Thesis. Monash University, Melbourne, Australia, 2004.

Boll, A., Hernández, R., 1986. Interpretación estructural del área de Tres Cruces. Boletín de Informaciones Petroleras. Tercera Época 3 (7), 2–14.

Bosio, P.P., Powell, J., del Papa, C., Hongn, F., 2009. Middle Eocene deformation-sedimentation in the Luracatao Valley: tracking the beginning of the foreland basin of northwestern Argentina. J. S. Am. Earth Sci. 28, 142–154.

Brandmeier, M., Wörner, G., 2016. Compositional variations of ignimbrite magmas in the Central Andes over the past 26 Ma, a multivariate statistical perspective. Lithos 262, 713–728.

Bywater-Reyes, S., Carrapa, B., Clementz, M., Schoenbohm, L., 2010. Effect of late Cenozoic aridification on sedimentation in the Eastern Cordillera of north-west Argentina (Angastaco basin). Geology 38, 235-238. https://doi.org/10.1130/G30532.1.

Breitkreuz, C., de Silva, S., Wilke, H.G., Jörg Pfänder, J.A., Rennod, A.D., 2014. Neogene to quaternary ash deposits in the coastal Cordillera in northern Chile: distal ashes from supereruptions in the central Andes. J. Volcanol. Geoth. Res. 269, 68–82. https://doi.org/10.1016/j.jvolgeores.2013.11.001.

Castellanos, A., 1950. El Uquiense. Sedimentos neógenos de Uquía (Senador Pérez) de la Provincia de Jujuy (Argentina): rosario, Universidad Nacional del Litoral, Facultad de Ciencias Matemáticas, Físico Químicas y Naturales. Ser. Técnico-Sci. 36, 1–56.

Coira, B., Kay, S.M., 1999. Evolución volcánica cenozoica de la región de Agua Escondida-Salar Aguas Calientes-Puna Austral (Andes Centrales 25°30′S). 14° Congreso Geológico Argentino. Actas 1, 90. Salta.

Coira, B., Malhburg Kay, S., Viramonte, J., 1993. Upper cenozoic magmatism of the Argentina Puna. Int. Geol. Rev. 35, 677–720.

Coira, B., Galli, C.I., Mahlburg Kay, S., Kay, R.W., Flores, P., 2014. Niveles piroclásticos como herramienta de correlación en los depósitos Cenozoicos del Grupo Payogastilla, Valles Calchaquí, Tonco y Amblayo, en el noroeste de Argentina. Rev. Asoc. Geol. Argent. 71 (2), 147–160.

Coira, B., Mahlburg Kay, S., Viramonte, J.G., Kay, R., Galli, C.I., C.I., 2018. Origin of late Miocene peraluminous Mn-rich garnet-bearing rhyolitic ashes in the andean foreland (northern Argentina). J. Volcanol. Geoth. Res. 364, 20–34. https://doi.org/10.1016/j.jvolgeores.2018.08.020.

Coira, B., Galli, C.I., Mahlburg Kay, S., Stockli, D.F., Flores, P., Eveling, E., 2022. Pliocene Pleistocene deposits of Humahuaca and Casa Grande basins, northwestern Argentina- key to understanding intermountain basins evolution. Andean Geol. 49 (2) https://doi.org/10.5027/andgeoV49n2-3377.

Coutand, I., Carrapa, B., Deeken, A., Schmitt, A.K., Sobel, E.R. y Strecker M.R., 2006. Propagation of orographic barriers along an active range front: insights from sandstone petrography and detrital apatite fission-track thermochronology in the intramontane Angastaco basin, NW Argentina. Basin Res. 18, 1–26.

Chesner, C.A., Rose, W.I., Deino, A., Drake, R., Westgate, J.A., 1991. Eruptive history of Earth's largest Quaternary caldera (Toba, Indonesia) clarified. Geology 19, 200–203.

de Silva, S.L., 1989. Geochronology and stratigraphy of the ignimbrites from the 21°30′S to 23°30′S portion of the Central Andes of northern Chile. J. Volcanol. Geoth. Res. 37, 93–131.

de Silva, S.L., 1991. Styles of zoning in central Andean ignimbrites; insights into magma chamber. In: Harmon, R.S., Rapela, C.W. (Eds.), Andean Magmatism and its Tectonic Setting, vol. 265. Geological Society of America Special Paper, pp. 217–232.

de Silva, S.L., Francis, P.W., 1989. Correlation of large ignimbrites—Two case studies from the Central Andes of northern Chile. Journal of Volcanology and Geothermal Research 37, 133–149. https://doi.org/10.1016/0377-0273(89)90066-8.

de Silva, S.L., Gosnold, W.A., 2007. Episodic construction of batholiths: insights from the spatiotemporal development of an ignimbrite flare-up. J. Volcanol. Geoth. Res. 167, 320–335.

de Silva, S.L., Zandt, G., Trumbull, R., Viramonte, J.G., Salas, G., Jimenez, N., 2006. Largescale silicic volcanism in the Central Andes, a tectonomagmatic phenomenon. Geol. Soc. London Spec. Publ. 269, 47–64.

de Silva, S.L., Bailey, J.E., Mandt, K.E., Viramonte, J.M., 2009. Yardangs in terrestrial1004 ignimbrites: Synergistic remote and field observations on Earth with applications to1005 Mars. Planetary and Space Science, 58 (4), 459–471.

Del Papa, C.E., Disalvo, A., Reynolds, J., Pereyra, R., Viramonte, J.G., 1993. Utilización de niveles piroclásticos en correlaciones estratigráficas: Un ejemplo para el Terciario. In: Superior del noroeste argentino. 12° Congreso Geológico Argentino y 2° Congreso deExploración de Hidrocarburos, Actas, 2. Asociación Geológica Argentina,Mendoza, pp. 166–171.

del Papa, C., Hongn, F., Petrinovic, I., Dominguez, R., 2004. Evidencias de deformación pre-miocena asociada al antepaís andino en la Cordillera Oriental (24° 35′ S- 66° 12′ O). Nota Breve. Rev. Asoc. Geol. Argent. 59, 5 06–509.

del Papa, C., Hongn, F., Powell, J., Payrola Bosio, P., Do Campo, M., Strecker, M.R., Petrinovic, I., Schmitt, A.K., Pereyra, R., 2013. Middle Eocene-Oligocene broken-foreland evolution in the Andean Calchaquí Valley, NW Argentina: insights from stratigraphic, structural and provenance studies. Basin Res. 25, 1-20. https://doi.org/10.1111/bre.12018.

Díaz, J. y, Malizzia, D., 1983. Estudio geológico y sedimentológico del Terciario Superior del valle Calchaquí (departamento de San Carlos, provincia de Salta). Boletín Sedimentol. 2, 8–28.

Fernández, J., Bondesio, P., Pascual, R., 1973. Restos de *Lepidosiren paradoxa* (Osteichthyes, Dipnoi) de la Formación Lumbrera (Eoceno, ¿Eogeno?) de Jujuy. Ameghiniana 10, 152–171.

Fernández-Turiel, J.L., Saavedra, J., Pérez-Torrado, J.F., Rodríguez-González, A., Carracedo, J.C., Osterrieth, M., Carrizo, J.I., Esteban, G., 2013. The Largest Holocene Eruption of the Central Andes Found. In: *en* American Geophysical Union Fall Meeting. American Geophysical Union, San Francisco, California, pp. V13D–V2639.

Folkes, C.B., de Silva, S., W right, H.M., Cas, R.A.F., 2011. Geochemical homogeneity of a long-lived large silicic system: evidence from Cerro Galan Caldera, NW Argentina. In: Cas, R.A.F y, Cashman, K. (Eds.), The Cerro Galán Ignimbrite and Caldera: Characteristics and Origins of a Very Large Volume Ignimbrite and its Magma System, vol. 73. Bulletin of Volcanology, Special Issue, New York, pp. 1455–1486.

Galli, C.I., Reynolds, J., 2012. Evolución paleoambiental del Grupo Payogastilla (Eoceno-Plioceno) en el valle Calchaquí-Tonco, provincia de Salta, Argentina. 13° Reunión Argentina de Sedimentología. Salta, Relatorio, pp. 67–80.

Galli, C.I., Hernández, R., Reynolds, J., 1996. Análisis estratigráfico del Subgrupo Metán (Grupo Orán), en el río Piedras, departamento Metán, Salta, Argentina. Boletín de Inform. Petrol. 12 (46), 99–107.

Galli, C.I., Ramirez, A., Reynolds, J., Viramonte, J.G., Idleman, B. y, Barrientos, C., 2011. Proveniencia de los depósitos del Grupo Payogastilla (Cenozoico), Río Calchaquí, provincia de Salta, Argentina. Rev. Asoc. Geol. Argent. 68, 263–278.

Galli, C.I., Coira, B., Alonso, R.N., Reynolds, J., Matteini, M., Hauser, N., 2014. Tectonic controls on the evolution of the andean cenozoic foreland basin: evidence from fluvial system variations in the Payogastilla group, in the Calchaquí, Tonco and Amblayo valleys, NW Argentina. J. S. Am. Earth Sci. 52, 234–259. https://doi.org/10.1016/j.jsames.2014.03.003.

Galli, C.I., Coira, B., Alonso, R.N., Iglesia Llanos, M.P., Prezzi, C., Kay, S., 2016. Tectonostratigraphic history of the Neogene Maimará basin, northwest Argentina. J. S. Am. Earth Sci. 72, 137–158. https://doi.org/10.1016/j.jsames.2016.09.007.

Galli, C.I., Alonso, R.N., Coira, L.B., Herrera Oviedo, P., 2017. Las cuencas de Antepaís cenozoicas de Cordillera oriental, Nroeste argentino. In: Muruaga, C., Grosse, P. (Eds.), Relatorio del XX Congreso Geológico Argentino (CGA. San Miguel de Tucumán. Universidad Nacional de Tucumán, ISBN 978-1-873671-00-9, pp. 213–240, 2017.

Gallardo, E.F., 1985. Estratigrafía y tectónica del cuaternario en la Cordillera Oriental de Salta y Jujuy. Informe Final CONICET (Salta) 88.

Galli, C.I., Alonso, R.N., Beamud Amorós, E., Pingel, H., Eveling, E., Coira, B.L., Stockli, D.F., González, D., 2021. Plio-pleistocene paleoenvironmental evolution of the intermontane Humahuaca basin, southern central Andes. J. S. Am. Earth Sci. 111, 103502. https://doi.org/10.1016/j.jsames.2021.103502.

Gauthier, P.J., Déruelle, B., Viramonte, J., Aparicio, A., 1994. Granats des rhyolites de la calderade La Pava-Ramada (NW Argentine) at de leursxénolites granitiques. Comptes Rendeus Acad. Sci. Paris 318 (serie II), 1629–1635.

Gebhard, J., Giudici, A.R., Oliver Gascon, J., 1974. Geología de la comarca entre el río Juramento y arroyo Las Tortugas, provincias de Salta y Jujuy, República Argentina. Rev. Asoc. Geol. Argent. 29, 359–375.

Glaze, L.S., Francis, P.W., Self, S., Rothery, D.A., 1989. The 16 September 1986 eruption of Lascar volcano, north Chile: satellite investigations, Bulletin. Volcanology 51, 149–160.

González, M.A., Tchilinguarian, P., Pereyra, F.X., Ramallo, E.E., y González, O.E., 2003. Hoja Geológica 2366-IV, ciudad de Libertador general san Martín. Provincias de Jujuy y Salta. In: Instituto de Geología y Recursos Minerales, Servicio Geológico Minero Argentino. Boletín 274. SEGEMAR, Buenos Aires.

Greene, L.L., 1995. Eolian Landforms in the Central Andes: Implications for the Long-Term Stability of Atmospheric Circulation. Unpublished M.S. Thesis. Cornell University, Ithaca, p. 62.

Grier, M.E., 1990. The Influence of the Cretaceous Salta Rift Basin on the Development of Andean Structural Geometries, NW Argentine Andes. Tesis de maestría, Cornell University, Ithaca, p. 178 (inédito).

Grier, M.E., Dallmeyer, R.D., 1990. Age of the Payogastilla Group. Implications for forenland basin development, NW Argentina. J. S. Am. Earth Sci. 4, 351–372.

Guzmán, S., Petrinovic, I., Brod, A., Hongn, F., Seggiaro, R., Montero, C., Carniel, R., Dantas, E., Sudo, M., 2011. Petrology of the Luingo caldera (SE margin of the Puna plateau): a middle Miocene window of the arc–back arc configuration. J. Volcanol. Geoth. Res. 200, 171–191.

Guzmán, S., Grosse, P., Montero-López, C., Hongn, F., Pilger, R., Petrinovic, I.A., Seggiaro, R., Aramayo, A., 2014. Spatial-temporal distribution of explosive volcanism in the 25-28°S segment of the Andean central volcanic zone. Tectonophysics 636, 170–189.

Hernández, R.M., Galli, C.I., Reynolds, J.H., 1999. Estratigrafía del Terciario en el noroeste argentino: Relatorio, vol. 1. XIV Congreso Geológico Argentino, Tomo, pp. 316–328.

Hongn, F., Seggiaro, R., 2001. Hoja Geológica 2566-III, cachi. Programa Natl. Cartas Geol. Repúbl. Argentina, Boletín 248, 1–87. Buenos Aires.

Kay, S.M., Coira, B.L., 2009. Shallowing and steepening subduction zones, continental lithospheric loss, magmatism, and crustal flow under the Central Andean Altiplano–Puna Plateau. In: Kay, S.M., Ramos, V.A., Dickinson, W.R. (Eds.), Backbone of the Americas: Plateau Uplift, Shallow Subduction and Ridge Collision. Geological Society of America Memoir 204. Geological Society of America, Boulder CO, pp. 229–259.

Kay, S.M., Maksaev, V., Moscoso, R., Mpodozis, C., Nasi, C., Gordillo, C.S., 1988. Tertiary Andean magmatism in Argentina and Chile between 28-33°S; Correlation of magmatic chemistry with a changing Benioff zone. J. S. Am. Earth Sci. 1, 21–38.

Kay, S., Coira, B., Viramonte, J., 1994. Young mafic back-arc volcanic rock as indicator of continental lithospheric delamination beneath the Argentine Puna plateau, Central Andes. J. Geophys. Res. 99 (B12), 24323–24339.

Kay, S.M., Mpodozis, C., Coira, B., 1999. Magmatism, tectonism, and mineral deposits of the Central Andes (22°–33°S latitude). In: Skinner, B.J. (Ed.), Geology and Ore Deposits Ofthe Central Andes, vol. 7. Society of Economic Geology Special Publication, pp. 27–35.

Kay, S.M., Coira, B., Mpodozis, C., 2006. Late Neogene volcanism in the Cerro Blanco region of the Puna austral Argentina, (∼26.5°S- ∼67.5°W). 11° Congreso Geológico Chileno, Actas 2, 499–502. Antofagasta.

Kay, S.M., Coira, B., 2008. Implications of chemical and isotopic variation in neogene Puna plateau ignimbrites for central andean crustal evolution. Goldscmidt Conference, Abstract A456.

Kay, S.M., Coira, B.L., Caffe, P.J., 2010. Regional chemical diversity, crustal and mantle sources and evolution of Puna plateau ignimbrites in the central Andes. J. Volcanol. Geoth. Res. 198, 81–111.

Kay, S.M., Coira, B., Wörner, G., Kay, R.W., Singer, S., 2011. Geochemical, isotopic and single crystal $^{40}Ar/^{39}Ar$ age constraints on the evolution of the Cerro Galán Ignimbrites. In: Cashman, K. y, Cas, R. (Eds.), Understanding a Super Volcano: the Cerro Galán Caldera and its Deposits,, vol. 73. Northwestern Argentina, Bulletin of Volcanology, Special Issue, USA, pp. 1487–1511.

Kley, J., Rossello, E.A., Monaldi, C.R., Habighorst, B., 2005. Seismic and field evidence for selective inversion of Cretaceous normal faults, Salta rift, northwest Argentina. Tectonophysics 399, 155–172. https://doi.org/10.1016/j.tecto.2004.12.020.

Kern, J., de Silva, S.L., Schmitt, A.K., Kaiser, J.F., Rodrigo Iriarte, A., Economos, R., 2016. Geochronological imaging of an episodically constructed subvolcanic batholith: U-Pb in zircon chronochemistry of the Altiplano-Puna Volcanic Complex. Geosphere 12, 4. https://doi.org/10.1130/GES01258.1.

Lindsay, J.M., Schmitt, A.K., Trumbull, R.B., de Silva, S.L., Siebel, W., Emmermann, R., 2001. Magmatic evolution of the La Pacana caldera system, Central Andes, Chile: compositional variation of two cogenetic, large-volume felsic ignimbrites. J. Petrol. 42, 459–486.

Lucassen, F., Becchio, R., Wilke, H.G., Thirlwall, M.F., Viramonte, J., Franz, G., Wemmer, K., 2000. Proterozoic– Paleozoic development of the basement of the Central Andes (18°-26°) a mobile belt of the South American craton. J. S. Am. Earth Sci. 13, 697–715.

Malamud, B.D., Jordan, T., Alonso, R.N., Gallardo, E., González, R., 1995. Four New Quaternary Ash and Tuff Ages, Lerma Valley, NW Argentina, vol. 22b. American Geophysical Union, Fall Meeting, p. 12.

Malamud, B.D., Jordan, T.E., Alonso, R.A., Gallardo, E.F., González, R.E., Kelley, S.A., 1996. Pleistocene Lake Lerma, Salta Province, NW Argentina, vol. IV. XIII Congreso Geológico Argentino y III Congreso de Exploración de Hidrocarburos, Actas, pp. 103–116.

Mamani, M., Wörner, G., Sempere, T., 2010. Geochemical variations in igneous rocks of the Central Andean orocline (13 S to 18 S): tracing crustal thickening and magma generation through time and space. Geol. Soc. Am. Bull. 122 (1–2), 162–182.

Marshall, L., Butler, R.F., Drake, R.E., Curtis, G.H., 1982. Geochronology of Type Uquian (late cenozoic) Land Mammal age, Argentina. Science 216 (Issue 454), 986–989. https://doi.org/10.1126/science.216.4549.986.

McPhie, J., Doyle, M., Allen, R., 1993. Volcanic Textures. A Guide to the Interpretation of Textures in Volcanic Rocks. Centre for Ore Deposit and Exploration Studies. University of Tasmania (Inedit), Tasmania, p. 198.

Montero-López, M.C., Hongn, F.D., Marrett, R., Seggiaro, R., Strecker, M., Sudo, M., 2010. Late Miocene-Pliocene onset of N-S extension along the southern margin of the Central Andean Puna plateau from magmatic, geochronological and structural evidences. Tectonophysics 494 (1–2), 48–63.

Ort, M., 1993. Eruptive processes and caldera formation in a nested downsag collapse caldera: Cerro Panizos, Central Andes Mountains. J. Volcanol. Geoth. Res. 56, 221–252. https://doi.org/10.1016/0377-0273(93)90018-M.

Ort, M., Coira, B.y, Mazzoni, M., 1996. Generation of a crust-mantle magma mixture: magma sources and contamination at Cerro Panizos, Central Andes. Contributions to Mineralogy and Petrology 123, 308–322.

Pascual, R., Vucetich, M.G., Fernández, J., 1978. Los primeros mamíferos (Notoungulata, Henricosbornidae) de la Formación Mealla (Grupo Salta, Subgrupo Santa Bárbara). Sus implicancias filogenéticas, taxonómicas y cronológicas. Ameghiniana 15, 366–390.

Petrinovic, I.A., Mitjavilla, J., Viramonte, J.G., Marti, J., Becchio, R., Arnosio, M., Colombo, F., 1999. Geoquímica y geocronología de las secuencias neógenas de trasarco, en el extremo oriental de la cadena volcánica transversal del Quevar, noroeste de Argentina. Acta Geol. Hisp. 34, 255–273.

Petrinovic, I.A., Riller, U., Brod, A., 2005. The Negra Muerta volcanic complex, southern Central Andes: geochemical characteristics and magmatic evolution of an episodic volcanic centre. J. Volcanol. Geoth. Res. 140 (4), 295–320. https://doi.org/10.1016/j.jvolgeores.2004.09.002.

Petrinovic, I.A., Martí, J., Aguirre-Díaz, G.J., Guzmán, S.R., Geyer, A. y, Salado Paz, N., 2010. The Cerro Aguas Calientes caldera, NW Argentina: an example of a tectonically controlled polygenetic collapse caldera, and its regional significance. J. Volcanol. Geoth. Res. 194, 15–26.

Pereyra, R., Becchio, R., Viramonte, J.G., Pimentel, M., 2008. Minerales pesados en depósitos piroclásticos de caída distales, su uso en la correlación crono-estratigráfica entre la Formación Angastaco (Grupo Payogastilla) y Formación Anta (Grupo Orán). In: Actas 17, vol. 1. Congreso Geológico Argentino, pp. 227–228. Jujuy.

Pingel, H., Strecker, M., Alonso, R.N., Schmitt, A., 2013. Neotectonic basin and landscape evolution in the eastern Cordillera of NW Argentina, Humahuaca basin (∼24°S). Basin Res. 25, 1–20. https://doi.org/10.1111/bre.12016.

Reynolds, J.H.C.I., Galli, C.I., Hernández, R.M., Idleman, B.D., Kotila, J.M., Hilliard, R.V., Naeser, C.W., 2000. Middle Miocene tectonic development of the Transition zone, Salta province, northwest Argentina: magnetic stratigraphy from the metan Subgroup, Sierra de Gonzalez. Geol. Soc. Am. Bull. 112 (11), 1736–1751.

Russo, A., 1972. La estratigrafía terciaria en el noroeste argentino. 5° Congreso Geol. Argentino, Actas 1, 1–14.

Russo, A., Serraiotto, A., 1978. Contribución al conocimiento de la estratigrafía terciaria en el noroeste Argentino. VII Congreso Geológico Argentino Actas I, pp. 715–730.

Salfity, J.A., Monaldi, C.R., 2006. Hoja Geológica 2566-IV, Metán. Programa Natl. de Cartas Geol. Repúbl. Argentina, SEGEMAR Boletín 319, 74. Buenos Aires.

Salfity, J.A., Gorustovich, S., Moya, C. y, Amengual, R., 1984. Marco tectónico de la sedimentación y efusividad cenozoicas en la Puna Argentina. IX Congreso Geológico Argentino, Actas 1, 539–554. San Carlos de Bariloche.

Salisbury, M.J., Jicha, B.R., De Silva, S.L., Singer, B.S., Jiménez, N.C., Ort, M.H., 2011. $^{40}Ar/^{39}Ar$ chronostratigraphy of Altiplano-Puna volcanic complex ignimbrites reveals the development of a major magmatic province. Geol. Soc. Am. Bull. 123 (5–6), 821–840.

Scasso, R.A., Corbella, H., Tiberi, P., 1994. Sedimentological analysis of the tephra from the12–15 August 1991 eruption of Hudson volcano. Bull. Volcanol. 56, 121–132.

Schmitt, A.K., de Silva, S.L., Trumbull, R., Emmermann, R., 2001. Magma evolution in the Purico ignimbrite complex, northern Chile: evidence for zoning of dacitic magmaby injection of rhyolitic melts following mafic recharge. Contrib. Mineral. Petrol. 140, 680–700.

Schnurr, W.B.W., Trumbull, R.B., Clavero, J., Hahne, K., Siebel, W. y Gardeweg M., 2007. Twenty-five million years of felsic magmatism in the southern Central Volcanic Zone of the Andes: geochemistry and magma genesis of ignimbrites from 25-27°S, 67-72°W. J. Volcanol. Geoth. Res. 166, 17–46.

Seggiaro, R., Hongn, F., Folguera, A., Clavero, J., 1999. Hoja Geológica 2769 – II, Paso de San Francisco, 1:250.000: Buenos Aires. Servicio Geológico Minero Argentino, Programa Nacional de Cartas Geológicas, 1 Mapa.

Seggiaro, R.E., Aguilera, N., Amengual, R., Boso, M., del Papa, C., Gallardo, E., Galli, C., Hongn, F., Marquillas, R., Ramallo, E., Sabino, I., 2019a. Hoja Geológica 2566-II, Salta. Provincias de Salta y Jujuy. Institut. Geol. Recursos Miner. Serv. Geológico Miner. Argentino. Boletín 440, 92. Buenos Aires.

Seggiaro, R., Guzmán, S., Martí, J., 2019b. Dynamics of caldera collapse during the Coranzulí eruption (6.6 Ma) (central Andes, Argentina). J. Volcanol. Geoth. Res. 374, 12. https://doi.org/10.1016/j.jvolgeores.2019.02.003.

Sobolev, S.V., Babeyko, A.Y., Koulakov, I., Oncken, O., Vietor, T., 2005. Mechanisms of the Andean orogeny: insights from numerical modelling. In: Oncken, O. (Ed.), The Andes. Frontiers in Earth Sciences. Springer, Berlin, Heidelberg. https://doi.org/10.1007/978-3-540-48684-8_25.

Sparks, R.S.J., Walker, G.P.L., 1977. The significance of vitric-enriched air-fall ashes associated with crystal-enriched ignimbrites. J. Volcanol. Geoth. Res. 2, 329–341.

Starck, D., Vergani, G., 2001. Desarrollo tecto-sedimentario del Cenozoico en el sur de la provincia de Salta. 13° Congreso Geológico Argentino, Argentina, pp. 433–452, 1996.

Starck, D., Anzotegui, L., 2001. The late Miocene climatic change persistence of a climatic signal through the orogenic stratigraphic record in north-western of Argentina. J. S. Am. Earth Sci. 14, 763–774. https://doi.org/10.1016/S0895-9811(01)00066-9.

Siks, B., Horton, B., 2011. Growth and fragmentation of the Andean foreland basin during eastward advance of fold-thrust deformation, Puna plateau and Eastern Cordillera, northern Argentina. Tectonics 30, TC6017. https://doi.org/10.1029/2011TC002944.

Streit, R., Burbank, D.W., Strecker, M., Alonso, R.N., Cottle, J.M., Kylander-Clark, A.R.C., 2015. Controls on intermontane basin filling, isolation and incision on the margin of the Puna Plateau, NW Argentina (∼23°S). Basin Res. 1–25. https://doi.org/10.1111/bre.12141.

Stingl, W., 1947. Estudio geológico de la zona de Casa Grande, departamento de Humahuaca, provincia de Jujuy. Universidad Nacional de Córdoba (Thesis), Córdoba.

Tait, M.A., 2004. Dynamics of a Large Volume Plinian Eruption: Dispersal of the Late Miocene Corte Blanco Tuff, Ramadas Volcanic Centre, Andes Mountains, Salta, Argentina (Ph.D. Thesis). Monash University, Melbourne, Australia, p. 254.

Tait, M.A., Cas, R.A.F., Viramonte, J.G., 2009. The origin of an unusual tuff ring of perlitic rhyolite pyroclasts: the last explosive phase of the Ramada Volcanic Centre, Andean Puna, Salta, NW Argentina. J. Volcanol. Geoth. Res. 183, 1–16.

Trumbull, R.B., Riller, U., Oncken, O., Scheuber, E., Munier, K., Hongn, F., 2006. Time-scales of magma formation, ascent and storage beneath sudbuction-zone volcanoes. In: Oncken, O., Chong, G., Franz, G., Giese, P., Götze, H.-J., Ramos, V.A., Strecker, M.R., Turner, S.P., George, R.M.M., Evans, P.J., Hawkesworth, C.J., Zellmer, G.F. (Eds.), The Time–Space Distribution of Cenozoic Arc Volcanism in the Central Andes: A New Data Compilation and Some Tectonic Considerations, vol. 358. Philos. Trans. R. Soc. Lond. A., pp. 1443–1464

Viramonte, J.G., Omarini, R.H., Araña Saavedra, V., Aparicio, A., García Cacho, I., Parica, R., 1984. Edad, génesis y mecanismos de erupción de las riolitas granatíferas de San Antonio de los Cobres, provincia de Salta. IX Congreso Geológico Argentino Actas 3, 216–233.

Viramonte, J.G., Reynolds, J.H., del Papa, C., Disalvo, A., 1994. The Corte Blanco garnetiferous tuff: a distinctive late Miocene marker bed in northwestern Argentina applied to magnetic polarity stratigraphy in the Río Yacones, Salta Province. Earth Planet Sci. Lett. 121, 519–531.

Viramonte, J.G., Arnosio, M., Becchio, R., de Silva, S., Roberge, J., 2008. Cerro Blanco volcanic complex, Argentina: a late Pleistocene to Holocene rhyolitic arc –related caldera complex in the central Andes. Int. Assoc. Volcanol. Chem. Earth's Interior vol. 1. International Association of Volcanologists and Chemistry of the Earth's Interior General Assembly, Reykjavík, Iceland.

Walther, A.M., Orgeira, M.J., Reguero, M., Verzi, D., Vilas, J.F., Alonso, R.N., Gallardo, E., Kelley, S., Jordan, T., 1998. Estudio paleomagnético, paleontológico y radimétrico de la Formación Uquía (Plio-Pleistoceno) en Esquina Blanca (Jujuy). Actas X Congreso Latinoamericano de Geología y VI Congreso Nacional de Geología Económica l, Buenos Aires.

Zandt, G., Leidig, M., Chmielowski, J., Baumont, D., Yuan, X., 2003. Seismic detection and characterization of the Altiplano-Puna magma body, central Andes. PAGEOPH Aki Symposium 160, 789–807.